Karlsruhe Institute of Technology

Annual Report 2020

Institute for Pulsed Power and Microwave Technology
Institut für Hochleistungsimpuls- und Mikrowellentechnik

John Jelonnek (ed)

Annual Report 2020

Institute for Pulsed Power and Microwave Technology
Institut für Hochleistungsimpuls- und Mikrowellentechnik

John Jelonnek (ed)

Part of this work was supported by ITER Organization under the task agreement C52TD53FE. The views and opinions expressed herein reflect only the authors views. The ITER Organization is not liable for any use that may be made of the information contained therein.

Part of this work has been carried out within the framework of the EUROfusion Consortium and has received funding from the Euratom research and training programme 2014-2018 and 2019- 2020 under grant agreement No. 633053. The views and opinions expressed herein do not necessarily reflect those of the European Commission. Parts of the simulations presented in this work have been carried out using the HELIOS supercomputer at IFERC-CSC.

Part of this work is supported by Fusion for Energy (F4E) under Grants F4E-GRT-553 and within the European GYrotron Consortium (EGYC). EGYC is a collaboration among SPC, Switzerland; KIT, Germany; HELLAS, Greece; IFP-CNR, Italy. The views expressed in this publication do not necessarily reflect the views of the European Commission.

Impressum
Karlsruher Institut für Technologie (KIT)

KIT – Die Forschungsuniversität in der Helmholtz-Gemeinschaft

Institute for Pulsed Power and Microwave Technology (IHM)

Institut für Hochleistungsimpuls- und Mikrowellentechnik (IHM)

Director: Prof. Dr.-Ing. John Jelonnek

The Institute for Pulsed Power and Microwave Technology (Institut für Hochleistungsimpuls- und Mikrowellentechnik (IHM)) is doing research in the areas of pulsed power and high-power microwave technologies. Both, research and development of high-power sources as well as related applications are in the focus. Applications for pulsed power technologies are ranging from materials processing to bioelectrics. High power microwave technologies are focusing on RF sources (gyrotrons) for electron cyclotron resonance heating of magnetically confined plasmas and on applications for materials processing at microwave frequencies.

The institute is doing research, development, academic education, and, in collaboration with the KIT Division IMA and industrial partners, the technology transfer. The reserach focus is on the long-term research goals of the German Helmholtz Association (HGF). The program-oriented research period (POF3) of HGF ended by end of the year 2020. In parallel a successful start of the new POF4 period is prepared. Still being in the POF3 period during 2020, the IHM was working in the research field ENERGY. Research projects were running within following four HGF programs: “Energy Efficiency, Materials and Resources (EMR)”; “Nuclear Fusion (FUSION)”, “Nuclear Waste Management, Safety and Radiation Research (NUSAFE)” and “Renewable Energies (RE)”. Starting with the new POF4 period, the IHM is continuing the research work in the HGF programs: “Nuclear Fusion (FUSION)” and “Nuclear Waste Management, Safety and Radiation Research (NUSAFE)”. The resources that were working in the HGF programs: “Energy Efficiency, Materials and Resources (EMR)” and “Renewable Energies (RE)” are moving into the new HGF program “Materials and Technologies for the Energy Transition (MTET)”.

During 2020, R&D work has been done in the following areas: fundamental theoretical and experimental research on the generation of intense electron beams, strong electromagnetic fields and their interaction with biomass, materials and plasmas; application of those methods in the areas of energy production through controlled thermonuclear fusion in magnetically confined plasmas, in material processing and in energy technology.

Mentioned long-term research areas require the profound knowledge on modern electron beam optics, high power micro- and millimeter waves, sub-THz technologies, vacuum electronics, material technologies, high voltage technologies and high voltage measurement techniques.

Table of Contents

Institute for Pulsed Power and Microwave Technology (IHM) Institut für Hochleistungsimpuls- und Mikrowellentechnik (IHM) **i**

Director: Prof. Dr.-Ing. John Jelonnek i

Table of Contents **iii**

1 Nuclear Fusion (FUSION): Plasma Heating Systems -Microwave Plasma Heating & Current Drive Systems- **5**

1.1 Gyrotron development for W7-X 6
1.2 Gyrotron development for ITER 9
1st phase of experimental verification of the 1 MW, 170 GHz updated CW gyrotron for ITER 9
1.3 Gyrotron development for DEMO 11
1.4 Progress in the development of the 2 MW, 170 GHz longer-pulse coaxial-cavity gyrotron 16
1.5 Experimental study of supression of parasitic oscillations in gyrotron beam tunnels 18
1.6 Code development 20
1.6.1 EURIDICE 20
1.6.2 New interaction code "SimpleRick" 20
1.7 Generation of ultra-short pulses with new gyro-devices 22
1.8 FULGOR (Fusion Long-Pulse Gyrotron Laboratory) 24
Journal Publications 26

2 Renewable Energy (RE): Bioenergy -Feedstocks and Pretreatment- **31**

2.1 PEF-processing of microbial biomass and industrial water streams 32
2.1.1 SABANA-Project: PEF-assisted cascade processing of microalgae 32
2.1.2 DiWaL: PEF-demo facility for PEF-treatment of electrodeposition paints 33
2.1.3 DiWaL: Bacterial decontamination of electro-dip paints by PEF-treatment 34
2.1.4 Anaerobic Digestion (AD) as final step for complete utilization of previously PEF-treated microalgal biomass 34
2.1.5 Lipid recovery from oleogenic yeast 36
2.1.6 Recovery of proteins from *Chlorella vulgaris* using PEF treatment 37
2.2 Components and electroporation processes 38
2.2.1 ZIM-Wine 38
2.2.2 Semiconductor-based Marx-type pulse generator for PEF-treatment of potatoes 39
2.3 Concentrating Solar Power (CSP)/ Liquid metal 40
2.3.1 GESA – SOFIE 40
2.3.2 Material development 41
2.3.3 Liquid metal battery 41
Journal Publications 42

3 Safety Research for Nuclear Reactors (NUSAFE): Transmutation -Liquid Metal Technology- **43**

3.1 Material development and advanced corrosion mitigation strategies for heavy liquid metal-cooled nuclear systems 44
3.1.1 Simulations of flow in the CORELLA facility 44
3.1.2 Material development to mitigate corrosion 45

4 Energy Efficiency, Materials and Resources (EMR): Energy-Efficient Processes -Multiphases and thermal processes- 46

4.1 Plasma chemistry 47
4.2 e-KOMFORT 48
4.3 High power solid-state microwave generators 49
4.4 Energy-efficient production of robust carbon fibers (REINFORCE) 50
4.5 Smart tomographic sensors for advanced industrial process control (TOMOCON) 51
4.6 Innovative microwave pultrusion for the cycle controlled sequential curing of fiber reinforced plastics for modular automated manufacture of complex components (IMPULS) 52
4.7 3D Microwave Printing of Composites 53
Journal Publications 54

Appendix 56

Equipment, Teaching Activities and Staff 56
Strategical Events, Scientific Honors and Awards 56
Longlasting Co-operations with Industries, Universities and Research Institutes 57

1 Nuclear Fusion (FUSION): Plasma Heating Systems -Microwave Plasma Heating & Current Drive Systems-

Contact: Dr. Gerd Gantenbein

The Department for High Power Microwave Technologies is focusing on the research and development of high power RF sources (gyrotrons) and related components for electron cyclotron resonance heating and current drive (ECRH&CD) of magnetically confined nuclear fusion plasmas. Additionally, it is involved in research and development in the field of and on the application of microwaves to chemical processes, materials and composites.

In particular the following major activities have been carried out in 2020:

- Gyrotron development for W7-X, targeting at 1.5 MW RF power at 140 GHz, a short-pulse gyrotron has been tested with a peak output power of appr. 1.6 MW, in depressed collector operation the efficiency was up to 44 %. Experiments on frequency stabilisation of a W7-X gyrotron by accelerating voltage tuning with a phase locked loop.
- Experimental tests with the improved European 1 MW, 170 GHz hollow-cavity gyrotron prototype for ITER, showed an output power of up to 1.2 MW in short-pulse operation, long pulse tests are ongoing.
- 2 MW, 170 GHz longer-pulse coaxial-cavity gyrotron prototype, further upgrade and conditioning of the modular short-pulse gyrotron, demonstration of 2 MW/11 ms and 1.5 MW/35 ms.
- Gyrotron development for DEMO, optimisation of the coaxial-cavity gyrotron for 170/204 GHz operation at 2 MW and start of manufacturing of components. Experimental investigations on advanced cooling concepts for cavities (mini-channel cooling). Studies on the feasibility of frequency-tunable Electron Cyclotron Wave (ECW) system for the suppression of Neoclassical Tearing Mode (NTM).
- Extensive study on the suppression of parasitic oscillations in gyrotron beam tunnels by modifying the beam tunnel ceramics.
- Upgrade of code-package EURIDICE to include external signal injection in interaction calculations, development of a software tool for the simulation of the electron-wave-interaction including a 3D electron beam (SimpleRick).
- Further elaboration of a new feedback system for a passive mode locked pulsed oscillator at 263 GHz in the frame of generation of ultra-short pulses with new gyro-devices.

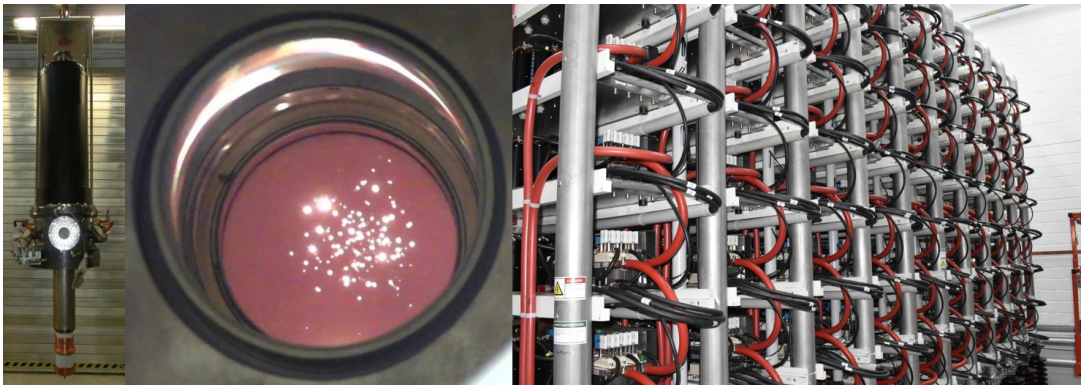

1.1 Gyrotron development for W7-X

Contact: Dr. Konstantinos Avramidis

The development of a Continuous-Wave (CW) 1.5 MW, 140 GHz prototype gyrotron for the upgrade of the ECRH system at W7-X is ongoing, within a contract between IPP and the industrial partner (Thales, Vélizy-Villacoublay, France). KIT/IHM is involved in the development within the framework of EUROfusion Work Package Stellarator 1 (WP S1). In parallel to the CW prototype, KIT has developed a short-pulse pre-prototype gyrotron (Fig. 1.1.1), which has identical RF and electron beam optics design with the prototype. Therefore, this gyrotron can allow for the experimental verification of the design in ms pulses, prior to the construction of the CW tube. Indeed, the baseline design of the 1.5 MW – 140 GHz gyrotron has been successfully validated in the 1st experimental campaign with the short-pulse pre-prototype. By operating the tube at different magnetic field it was possible to demonstrate output power of 1.6 MW with 30 % efficiency in non-depressed collector operation. In depressed collector operation the efficiency of the tube was increased to 44% for the nominal power of 1.5 MW, whereas it surpassed 46 % for 1.1 MW pulses. Results at nominal power and depressed collector operation are shown in Fig. 1.1.2. Despite that there have been cases where parasitic signals were excited (as expected for short pulses due to the optimization of the electron gun for CW operation) it was possible to find a wide parameter range for parasitic-free, high-efficiency operation. Nevertheless, further experiments are planned with a second assembly of the short-pulse tube with an optimized alternative beam-tunnel, targeting at a wider parameter range of parasitic-free operation.

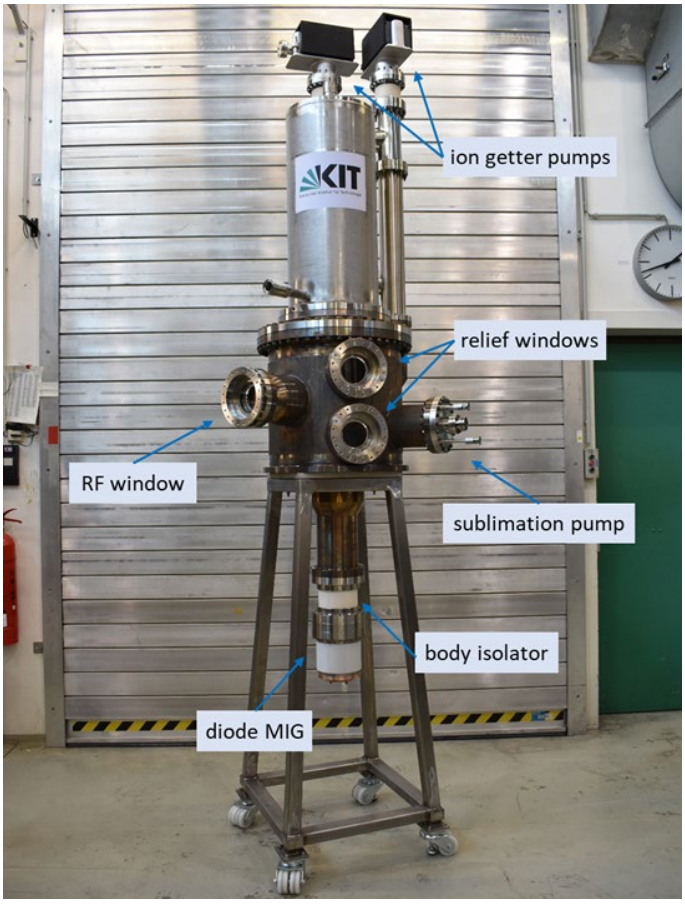

Fig. 1.1.1: The first assembly of the 1.5 MW – 140 GHz short-pulse pre-prototype gyrotron.

Following the successful 1st experimental campaign, a Critical Design Review (CDR) Meeting took place in October 2020, where the design of the CW gyrotron was approved, save for the cavity cooling circuit and the beam tunnel. The design of the cooling circuit was finalized later, following a series of multi-physics studies in collaboration with Politecnico di Torino. The decision between the baseline or the alternative beam tunnel as well as the complete approval of the design is foreseen in Q2 2021, after the completion of the 2nd experimental campaign with the short-pulse gyrotron. The CW tube delivery is scheduled for Q4 2021 and the Site Acceptance Tests will follow at KIT.

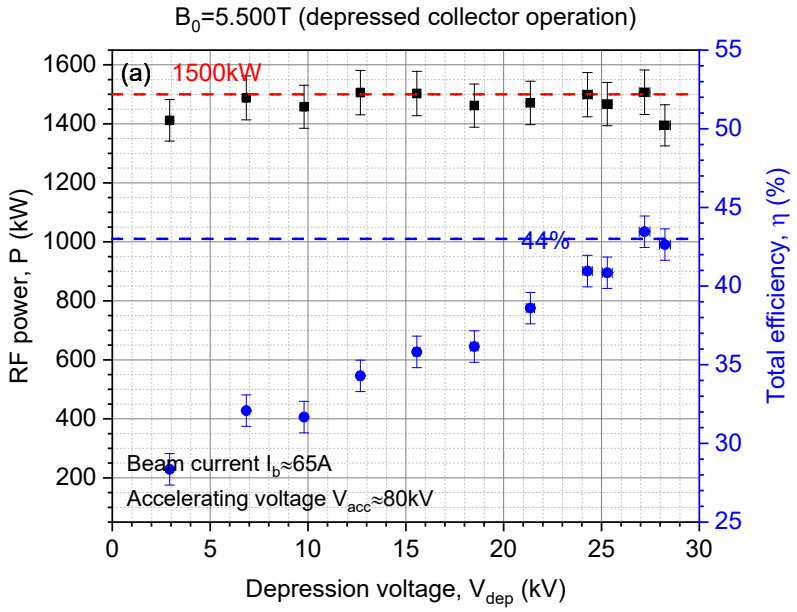

Fig. 1.1.2: High-efficiency depressed-collector operation at nominal 1.5 MW power, achieved in 1 ms pulses with the first assembly of the 1.5 MW – 140 GHz short-pulse gyrotron.

In view of the development of a new 175 GHz Collective Thomson Scattering (CTS) diagnostic at W7-X, a new 7 T magnet is required. The magnet proposals from three suppliers were extensively analysed, in terms of gyrotron performance at 140 GHz and 175 GHz, and were found to be suitable. In parallel, since CTS is highly benefited by a stable frequency, theoretical studies towards frequency stabilization of gyrotrons through an external control circuit were conducted. A Phase Locked Loop (PLL) circuit for the gyrotron was analysed in the control theoretical context, and a loop filter was determined to guarantee the stability of the PLL circuit. A schematic of the used principle is shown in Fig. 1.1.3. The possibility of gyrotron frequency stabilisation was then demonstrated by simulation and the physical realization of the control circuit is ongoing. This will be the first time that such a frequency stabilization scheme will be applied to MW-class gyrotrons.

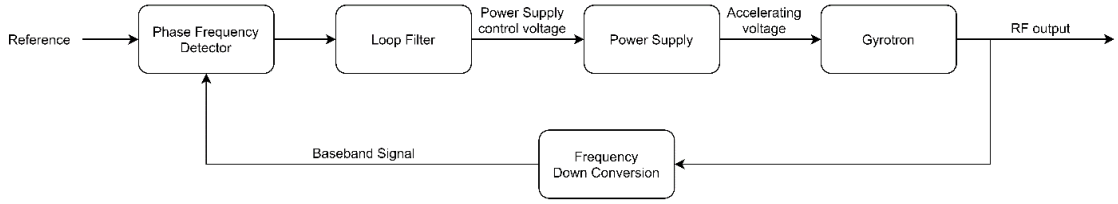

Fig. 1.1.3: Principle of the gyrotron frequency stabilization.

1.2 Gyrotron development for ITER

Contact: Dr. Tomasz Rzesnicki

1st phase of experimental verification of the 1 MW, 170 GHz updated CW gyrotron for ITER

After first experimental campaign in 2016, the improved 1 MW, 170 GHz, CW gyrotron (TH1509U) was delivered in July 2020 for tests at KIT. Two important aspects have been addressed and improved. In particular, (1) proper generation of a uniform election beam (emitter alignment) and (2) limitations on the body high voltage stand-off was improved by modification of the HV feedthroughs. It was found that the gyrotron position with respect to the magnetic field is misaligned by about 0.37 mm (excitation circle method), which can be compensate by the dipole coil system of the magnet. The excitation circles were circular and did not show any deformations, indication a very good mechanical alignment of the gyrotron components. Furthermore, the voltage stand-off properties of the gyrotron were tested as well, with the gyrotron installed inside the cryostat and fully prepared for CW operation. The measurements were performed both with and without activated magnetic field. During the tests, it was possible to apply more than 90 kV to the cathode with the body grounded as well as 40 kV to the body with the cathode grounded which was much better compared with the results from 2016.

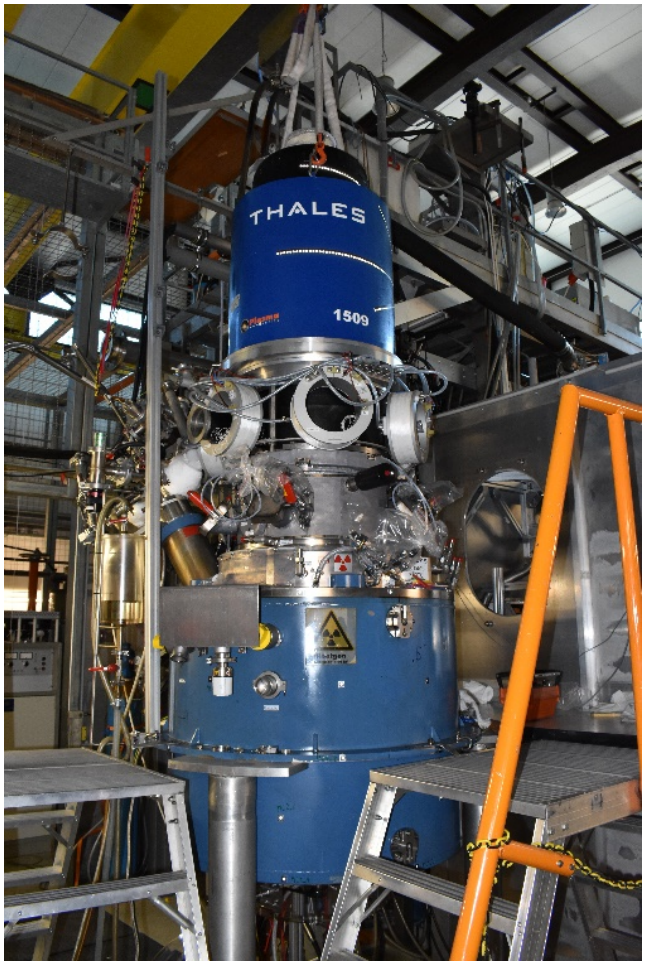

Fig. 1.2.1: 1 MW, 170 GHz .CW gyrotron installed in the test stand at IHM/KIT

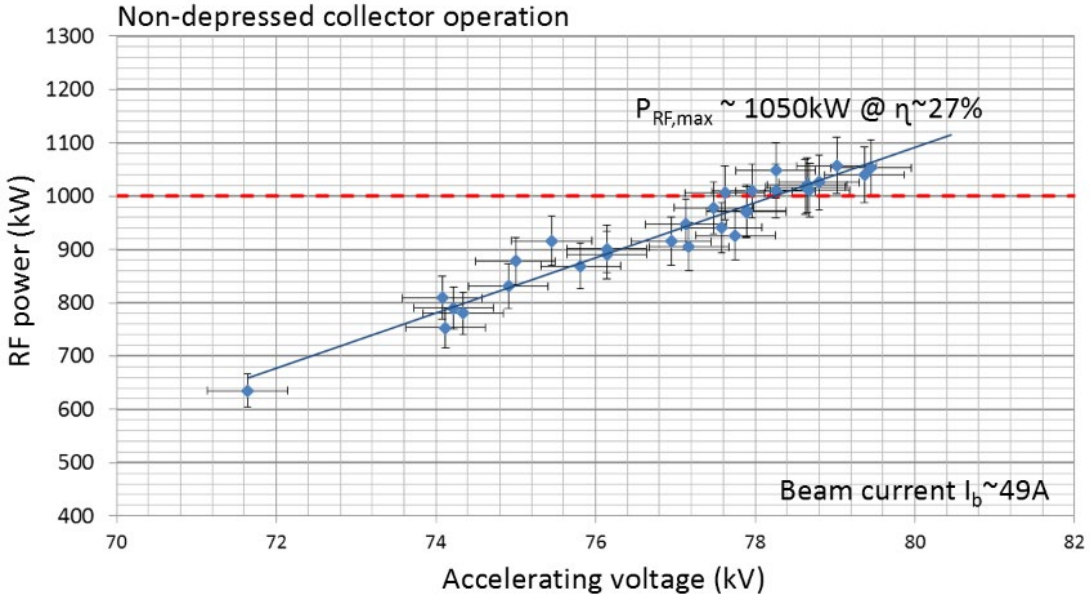

Fig. 1.2.2: Generated RF output power vs. accelerating voltage.

In the first phase of the experiments, a focus was on short-pulse characterisation of the TH1509U gyrotron in order to have a direct comparison with the results achieved in 2016. In frame of these activities, the electron beam was aligned to the centre of the in the cavity, using the dipole-coils and a complete operational map in Low Voltage Operating Point (LVOP) was recorded with 1 ms pulses. The maximum power that was recorded in the map for non-depressed collector operation is P_{RF} = 1050 kW with accelerating voltage U_{acc} = 79.8 kV and beam current I_b = 49 A. The measured RF output power versus the accelerating voltage is presented in Fig. 1.2.2. In addition, by increasing of the beam current and some optimization on the magnetic field configuration, it was possible to increase the generated power level to approx. 1.2 MW, keeping the efficiency around 26 %. Next, the test stand was prepared for CW operation and further conditioning procedure of the gyrotron (incl. collector cleaning) was started. The 2nd phase of the experiments, related to the long-pulse operation, will start in January 2021.

1.3 Gyrotron development for DEMO

Contact: Dr. Konstantinos Avramidis

The R&D related to the gyrotron for DEMO is in line with the European Fusion Roadmap towards a demonstration power plant and it is performed, at the largest part, within the Work Package Heating and Current Drive (WPHCD) of EUROfusion. The current European DEMO1 baseline poses significant challenges on the gyrotron. These are the need for dual, high-frequency operation (170/204 GHz) and/or fast frequency step-tunability, as well as the requirements for higher power (2 MW), higher overall efficiency (≥ 60 %), and a higher level of reliability and industrialisation, in line with that of a power plant. To keep the gyrotron R&D relevant with respect to possible baseline changes and to alternative reactor configurations towards a future power plant, efficient MW-class gyrotron operation at higher (>200 GHz) frequencies is also considered in parallel.

The advanced concept of the coaxial gyrotron has been selected as being the most promising, compared to the conventional hollow-cavity gyrotron, towards the higher power and frequency targets. The next step for coaxial gyrotron technology towards DEMO is to prove experimentally its capability for long-pulse operation. To this end, a first configuration of a longer-pulse 170 GHz, 2 MW coaxial-cavity gyrotron has been developed at KIT. The goal of this configuration is to be able to extend the pulse length up to ~100 ms, provided that an axial sweeping system is used for the collector. Following the successful extension of the pulse length with this gyrotron up to 10 ms/1 MW in the previous period, the short-pulse calorimeter was replaced by a longer-pulse load in order to extend the pulse length further (Fig. 1.3.1-left). With this set-up, it was possible to achieve pulse lengths above 30 ms at power levels of 1.4 MW, as shown in Fig. 1.3.1–right. In parallel, it was possible to generate more than 2 MW of output power with total efficiency 47 % during 11 ms pulses. Additional conditioning of the tube is required before further increase of the pulse length.

To keep the path towards the DEMO gyrotron as fast and cost-effective as possible, the development of a short-pulse dual-frequency 170/204 GHz 2 MW coaxial gyrotron is ongoing, using the existing 170 GHz, 2 MW coaxial gyrotron as a starting point. A modification of the existing anode design was made, which is necessary to allow the operation of the gyrotron in the magnetic field profile of the new 10.5 T superconducting magnet. The modified anode is shown in Fig. 1.3.2. The simulated electron beam parameters with this anode satisfy the requirements for the beam quality. The subsequent interaction simulations using these parameters showed an RF output power of 2.54/2.08 MW with an interaction efficiency of 38.8 %@170 GHz and 34.3 %@204 GHz, respectively. In parallel, the theoretical studies on step-tunability of the gyrotron frequency in a bandwidth of ±10 GHz and in steps of 2-3 GHz at 170 GHz and 204 GHz were continued, in support of a frequency-tunable Electron Cyclotron heating system (discussed later in this chapter). The excessive Ohmic loading of the coaxial insert, which was identified as a critical issue in the previous period, was mitigated by the proposal of a new mode series for tuning around both centre frequencies. With the new mode serie the insert loading remains at the acceptable levels.

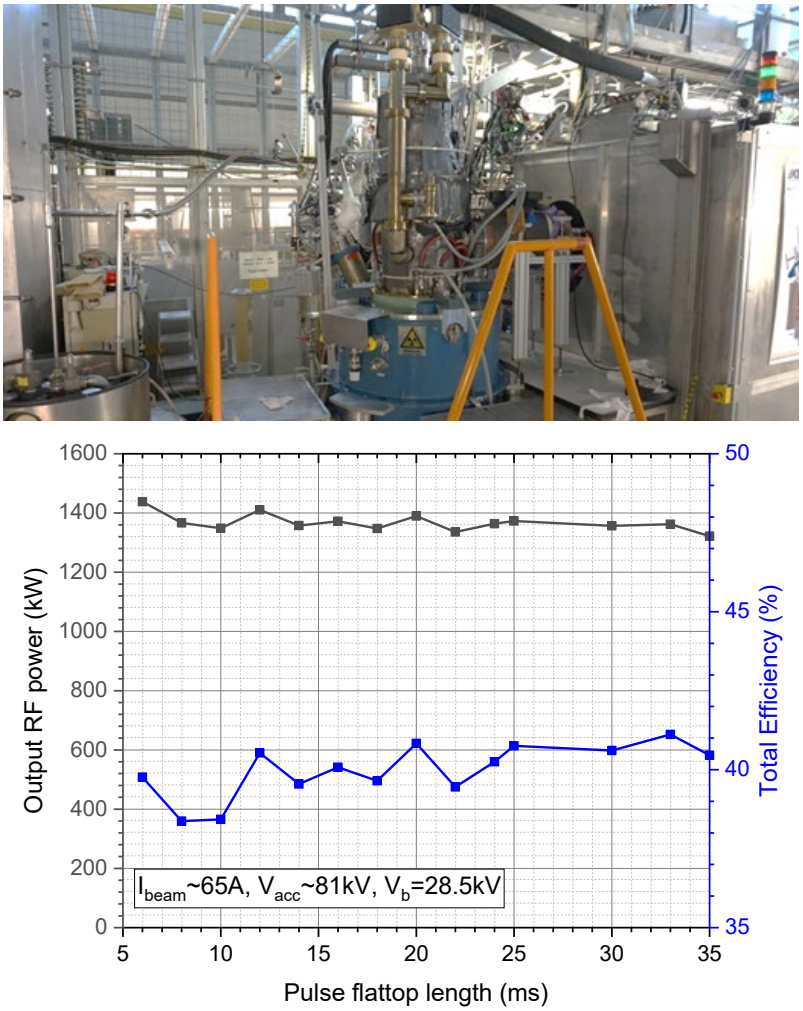

Fig. 1.3.1: Experimental set-up of the coaxial gyrotron with the longer-pulse load installed (top), and achieved pulse-length extension up to 35 ms (bottom).

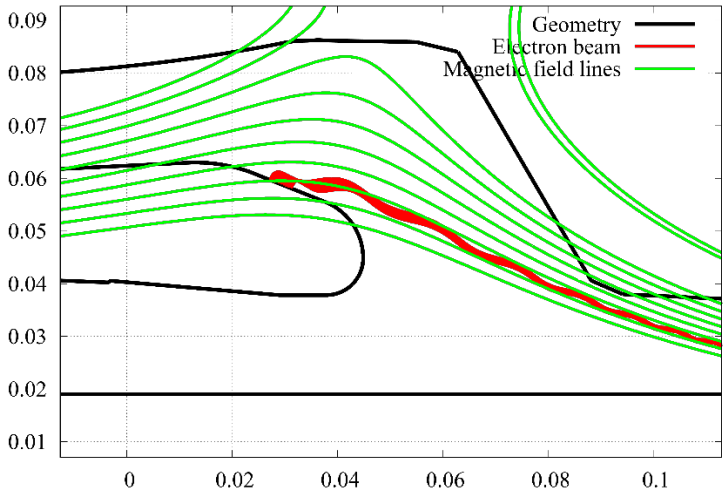

Fig. 1.3.2: Schematic of the modified geometry of the anode of the coaxial Magnetron Injection Gun.

With respect to all the components necessary for the first experiments with the dual-frequency gyrotron, the technical drawings have been prepared and the manufacturing process has started. The components include the modified anode, a new longer coaxial insert, adapters, an X-Y-table, and the oil tank. In order to support the experiment, the frequency diagnostic systems must also be upgraded up to 260 GHz, since the current limitation is at 175 GHz. The Frequency Measurement System (FMS) has been upgraded and tested in the laboratory (Fig. 1.3.3). In addition, the upgrade of the Pulse Spectrum Analysis (PSA) system has started: the harmonic order has been chosen and the required components have been ordered.

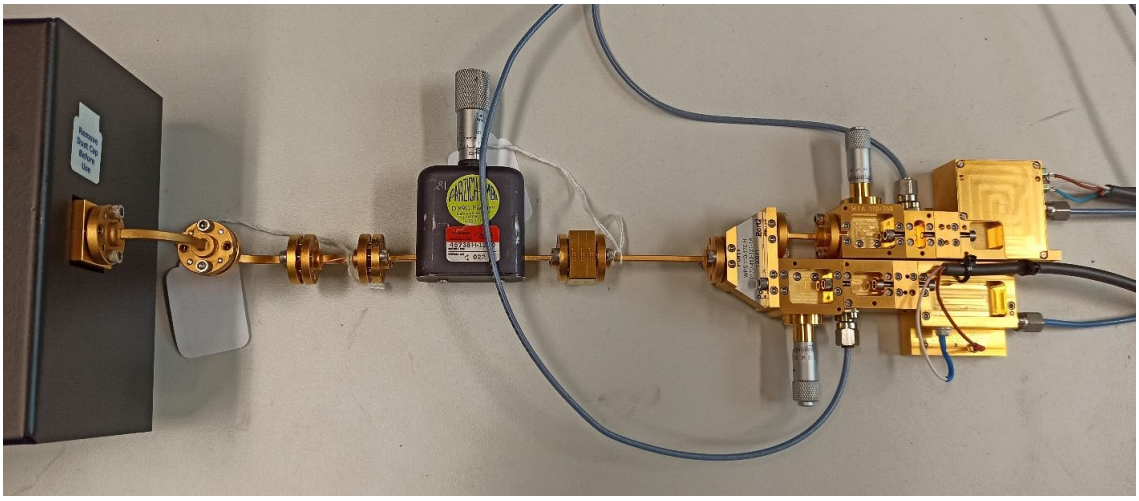

Fig. 1.3.3: Setup of the first test in the laboratory of the FMS system for frequency detection from 110-260 GHz.

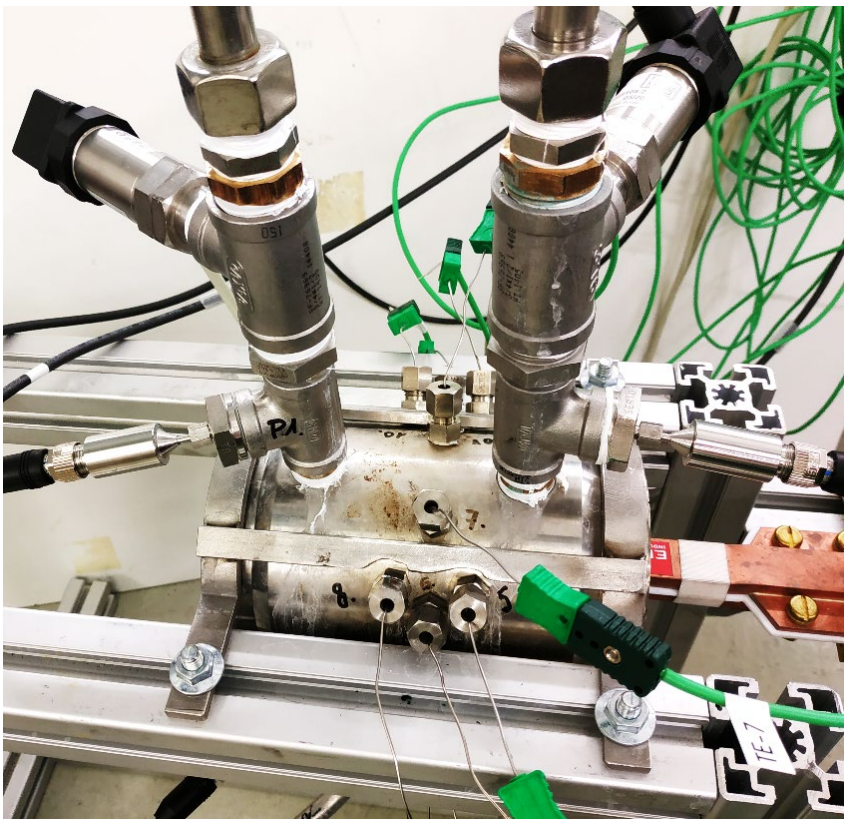

Fig. 1.3.4: Mini-channel mock-up, thermal sensors (green), pressure sensors (black), and inductor heater head (red).

Since the maximum acceptable heat-load on the cavity wall of fusion gyrotrons is a technological limiting factor for power, efficiency, and pulse-length, studies on advanced cooling systems are ongoing. A mock-up cavity, relevant to the 170 GHz, 2 MW coaxial gyrotron and equipped with a mini-channel cooling configuration, has been tested in the existing test set-up (Fig. 1.3.4). This set-up uses an advanced induction heating system to emulate the concentrated heat-load profile in the gyrotron cavity. The numerical evaluation of the experimental results was done in collaboration with Politecnico di Torino, Italy, who performed the 3D thermal-hydraulic simulations. First heating experiments using the mock-up without cooling focused on determining the appropriate calibration factors to reconcile the experimental temperatures with those computed by thermal 3D simulations, which use as input the induced heat load estimated by an electromagnetic model. Following that, calorimetry tests with different flow rates of the coolant and different inductor power levels were performed. The measured results match well with those of 3D thermal-hydraulic simulations. Hence, the simulation procedure and calibration can be now considered robust and can be used for future interpretation of the experimental results at more relevant parameters.

The target of ≥ 60 % efficiency for the DEMO gyrotron implies the development of advanced, Multi-Stage Depressed Collectors (MDC) to increase the energy recuperation from the spent electron beam. The theoretical studies related to the development of an MDC system for high power gyrotron based on **E×B** drift concept were continued. The compact MDC design developed in the previous period was modified to be compatible with the short-pulse dual frequency 170 GHz/204 GHz coaxial-cavity gyrotron in the new 10.5 T superconducting magnet. Even if the MDC design was optimized for operation at 170 GHz, the same design provides a satisfactory operation also at 204 GHz. Based on the scientific design, engineering drawings of the MDC system for the dual frequency gyrotron were prepared (Fig. 1.3.5) and the detailed manufacturing drawings are in progress. Several critical sub-components for the first prototype MDC have already been ordered. The manufacturing of additional sub-components is starting soon at KIT. In parallel, a testing plan for the experimental validation of the **E×B** drift MDC principle in FULGOR has been proposed. Theoretical studies for the upgrade of the MDC design to operate in Continuous Wave (CW) were also initiated: a concept for a CW compatible design approach was developed with an acceptable power loading density.

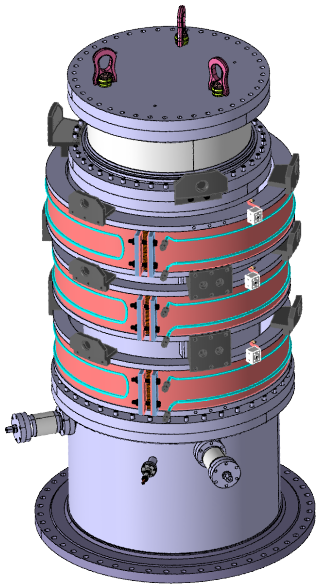

Fig. 1.3.5: 3D model of the mechanical design of the complete prototype MDC for the dual frequency gyrotron.

In parallel to the gyrotron development for DEMO, the feasibility study of using a frequency-tunable Electron Cyclotron Wave (ECW) system for the suppression of Neoclassical Tearing Mode (NTM) in DEMO is continued in the framework of a dedicated EUROfusion Engineering Grant. The previous numerical implementation of the modified Rutherford equation has been revised in order to obtain more proper estimations of the growth and stabilization behaviors of NTMs. Parameters (plasma current, magnetic field, plasma shape, safety factor, density, temperature, etc.) from the current reference DEMO baseline are considered in the setup of the plasma scenario. More important, instead of the analytically shifted and scaled ECW profiles, the deposition power density and current-drive profiles in the new simulations are numerically calculated by a beam tracing code (TORBEAM) simultaneously with the equilibrium (by SPIDER) and plasma transport in ASTRA calculations. In this way, the estimated current drive is more realistic than the fitted analytical assumptions. The same ECW launching position as in the current DEMO design are considered for the frequency-tunable system, while the launching angles are optimized for the frequency tuning such that the tuning steps could cover the vicinity of the targeted plasma rational surfaces without too much reduction of current drive efficiency. A schematic of the launching positions/angles is shown on Fig. 1.3.6.

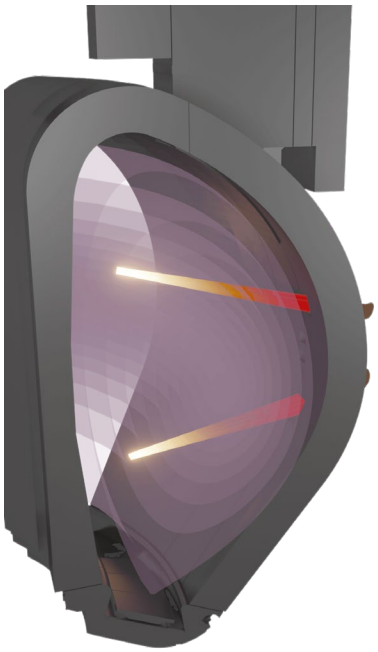

Fig. 1.3.6: Schematic of ECW beams (red) and flux surfaces in DEMO.

1.4 Progress in the development of the 2 MW, 170 GHz longer-pulse coaxial-cavity gyrotron

Contact: Dr. Tomasz Rzesnicki

KIT is developing a longer-pulse coaxial-cavity gyrotron with the goal of generating 2 MW of power at 170 GHz with pulse duration of up to 100 ms in the first step and up to 1 s after a second round of modifications. During the previous years, multiple upgrades have been introduced to the standard short-pulse pre-prototype construction of the gyrotron. In brief, the key components of the tube have been equipped with cooling systems, a new triode Magnetron Injection Gun has been manufactured, the collector flange has been adapted in order to accommodate a HELICOFLEX sealing and, finally, a trajectory correction coil was installed on the collector to control the body current of the tube. After the above listed modifications, the gyrotron was for the first time properly baked-out in a Nitrogen oven and an excellent vacuum quality has been achieved. During the first period of the experiments, it was possible to demonstrate 1 MW@10 ms, 1.5 MW@7 ms and 2 MW@5 ms pulses. In order to continue the experiments with longer pulses, a middle-pulse load (Fig. 1.4.1) was installed It dissipates 2 MW for up to 250 ms.
Considering the necessary conditioning of the tube for the pulses longer than 10 ms and taking into account some limitation related to the gyrotron collector and output window, that was not upgraded yet, it was decided to operate the gyrotron at the lower power level of 1.5 MW and to not extend the pulse length of 50 ms, first. The optimal performance of the gyrotron, in terms of output power was achieved at 26.5 kV of depression voltage, where more than 1.5 MW are generated with >42 % of total efficiency. An example of the profile of the pulse is presented in Fig. 1.4.2. In addition, a stable operation at RF power level of 1 MW at pulse lengths up to 50 ms, was demonstrated.

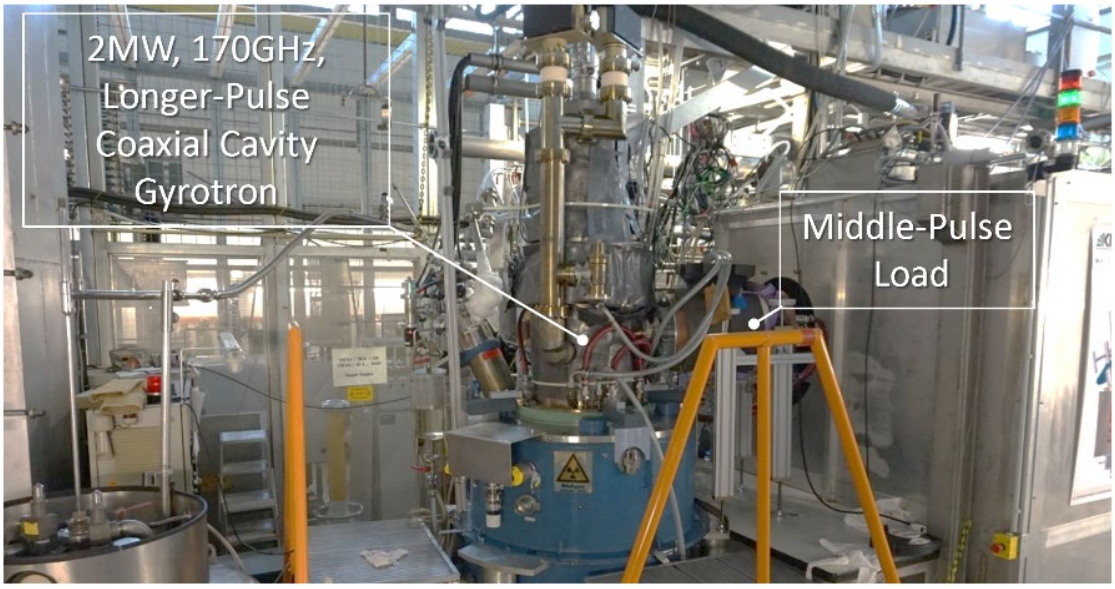

Fig. 1.4.1: 2 MW, 170 GHz, Longer-Pulse Coaxial-Gyrotron after installation.

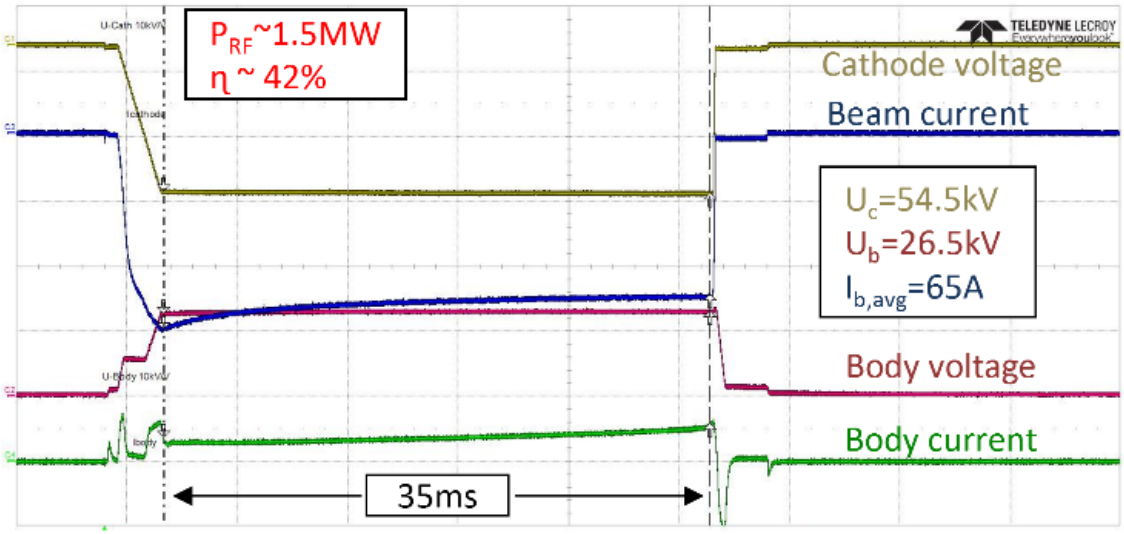

Fig. 1.4.2: 1.5 MW operation at 35 ms - pulse profiles example.

The gyrotron has been also successfully operated at 2 MW operating points with pulses up to 11 ms. For the first time the advantage of the triode gun was used. In order to be able to control the electron's pitch factor, the modulation anode is not grounded this time and voltage up to U_{mod} = -4 kV is applied by using a DC power supply. At those conditions, it was possible to generate more than 2 MW of power with total efficiency close to 47 %.

As the next step, a full upgrade to the long-pulse configuration is planned, in particular, a long-pulse collector incl. dedicated sweeping system, as well as cooled diamond output window will be installed. In addition, some improvements in the construction of the electron gun are in progress.

.

1.5 Experimental study of supression of parasitic oscillations in gyrotron beam tunnels

Contact: Dr. Tomasz Rzesnicki

High-power gyrotrons may suffer from parasitic oscillations that are excited in the electron-beam compression zone. Different damping structures are introduced and currently under experimental verification. The main goal is to reduce the possibility of parasitic excitation by increasing the starting currents of the modes. Dedicated experiments were performed by using a modular 170 GHz, 1 MW short-pulse gyrotron, which, due to its flanged construction, gives the possibility to modify the beam tunnel without affecting the rest of the tube. Based on the first experimental results done previously with a "standard" beam, the observed parasitic oscillation have been divided into two groups according to their frequency values and possible occurrence areas. Parasitic oscillations observed at frequencies (1) 146-148 GHz were consider to be excited in the beam tunnel area and (2) 151-161 GHz these find their origin in so called spacer area, which consists of a metallic conical element without dielectric rings. A theoretical study shows that a significant increase of the absorption of the dielectric material can be achieved by using materials with relatively low values of the real and imaginary parts of the permittivity. An accordantly modified beam tunnel (Fig. 1.5.1) structure has been tested at first giving very encouraging results. By replacing of the BeOSiC material composition of the last five dielectric rings of the beam tunnel with reduced SiC content from 40 % to 5 %, it was possible to increase the starting current of the parasitic oscillation and extend the stable range of the gyrotron operation. Fig. 1.5.2 shows gyrotron operational maps, where the measured power with respect to of the magnetic field profile parameters (emitter angle and radius in cavity) is presented. Additionally, the existence of the above mentioned types of the parasitic oscillation were presented, for two different beam tunnel setups (a) of a standard one (left) and (b) with new kind of ceramics (right). The results conformed a significant reduction of the parasitic oscillations activity and an extending of the highest-power excitation areas, in case of the beam tunnel with improved ceramic material composition.

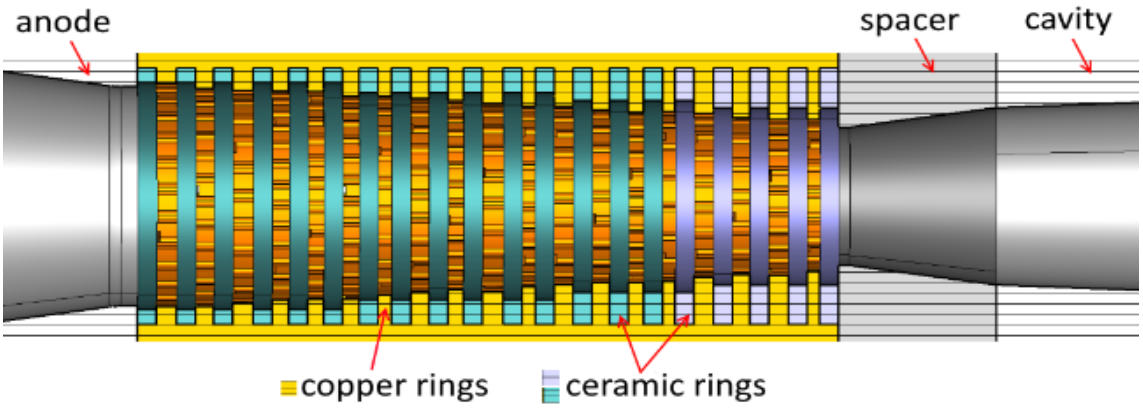

Fig. 1.5.1: Improved beam tunnel design.

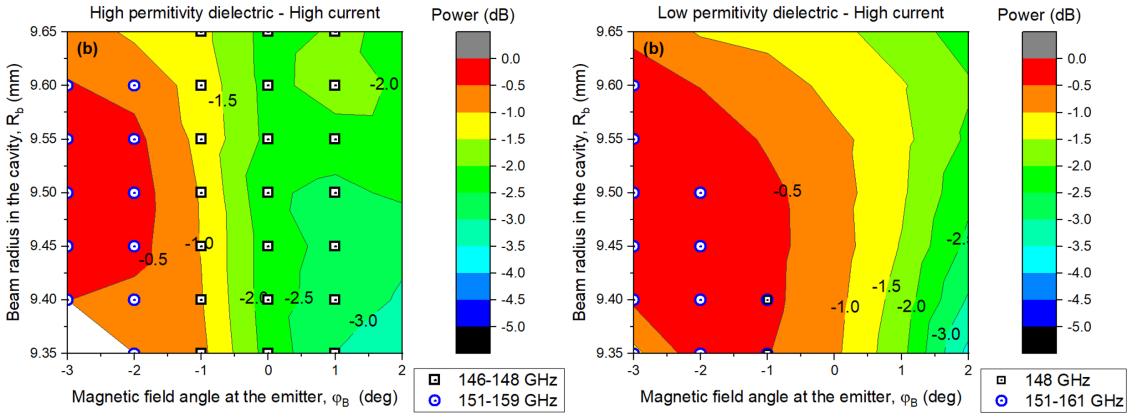

Fig. 1.5.2: Comparision of the results achieved at higher operating currents (~54 A) with the "standard" beam tunnel (left) and after replacement of last five beam tunnel ceramic rings with lower permitivity values (right).

Furthermore, in order to suppress the frequencies at 151-161 GHz, a modified version of the beam tunnel, with damping ceramic loaded spacer area was prepared and tested. In such configuration an additional increase of the starting current, by more than 10 % for all operating points was observed.
Further investigation of the optimized beam tunnel construction in order to suppress of unwanted oscillation is in progress.

.

1.6 Code development

Contact: Dr. Konstantinos Avramidis

1.6.1 EURIDICE

By injecting a low-power signal, of the order of -20 dB below the nominal power, it is possible to lock the gyrotron frequency to that of the external signal, provided that the frequency of the signal lays within a specific locking bandwidth around the operating frequency of the free-running gyrotron. In this way, full control of the gyrotron frequency can be achieved opening new possibilities in fusion diagnostics, spectroscopy, radar etc. In addition, the injected signal can strengthen the operating mode of the gyrotron against competition from other modes and therefore enhance the stability of the device. To address the effects of external signal injection in the gyrotron, the interaction model in the code-package EURIDICE for gyrotron interaction simulations and cavity design has been upgraded accordingly, in order to include the external signal. Initial benchmarking of this new feature has shown excellent behavior of the code and agreement with the theoretical predictions. Illustrative results are shown in Fig. 1.6.1.

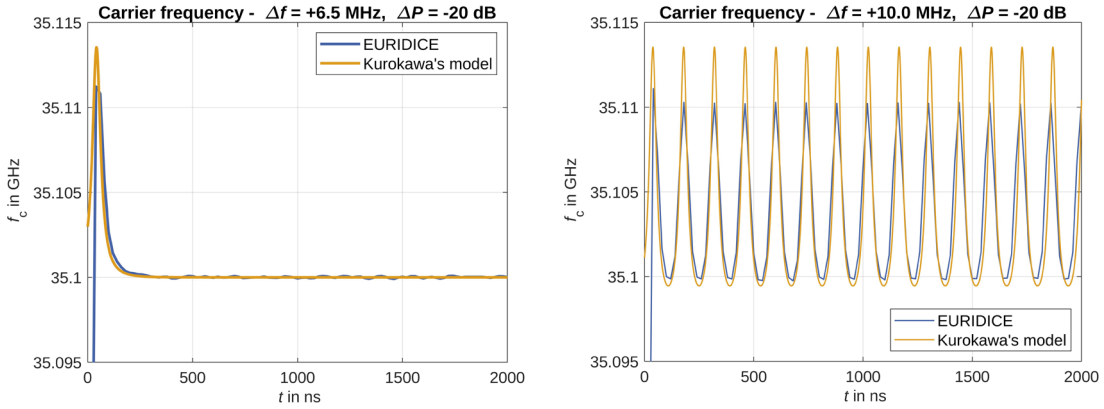

Fig. 1.6.1: Comparison of EURIDICE results with the theoretical results from Kurokawa, for a gyrotron with 35.1065 GHz free-running frequency. Left: injection at 35.1000 GHz (within the locking band), resulting in frequency locking at 35.1000 GHz. Right: injection at 35.0965 GHz (outside the locking band), resulting in absence of locking and appearance of beating.

1.6.2 New interaction code "SimpleRick"

The existing approaches for the simulation of the non-linear beam-wave interaction in gyrotron devices can be categorized into two groups: The first group consists of PIC-codes which usually include a 3D description of the particle motion and a full-wave simulation of the RF-field. These programs are designed for universal application and are suitable for the simulation of almost all types of vacuum tubes. E.g. the commercial software packages CST Microwave Studio and MAGIC belong to this group. Their disadvantage is the required high computing effort and, the high amount of memory. The second group consists of programs using simplified physical models. For the transient simulation of gyrotron devices, the models are often based on the slowly varying amplitudes approach. Several implementations for the transient simulation of gyro-devices are developed and published during the last 5 decades. They differ mainly in their handling of the electron beam, the modeling of the electron-wave interaction and the applied numerical methods.

In the frame of a PhD thesis, a new alternative model, named "SimpleRick", for the simulation of the electron-wave interaction in gyro devices is developed. It is also based on the approach of slowly varying amplitudes but includes a 3D electron beam and a source term derived for an arbitrary electron beam without restriction of the generality. The proposed model provides a number of advantages: It allows the simulation of electron beams with arbitrary particle distributions e.g. velocity spread, energy spread, offset of the guiding center from the symmetry axis of the device, etc. In addition, the consideration of inhomogeneities or misalignment of the static magnetic field is possible. A direct usage of simulation results e.g. from electron gun simulations is possible and it simplifies the interface to specialized simulation tools for the simulation of the electron beam behavior in the structures following the interaction space, e.g. the collector. The individual handling of macro particles in the beam enables the inclusion of additional physical effects as e.g. influences of space-charge fields. Additionally, the general formulation of the source term allows an electron-wave interaction at arbitrary harmonics which can be important for the investigation of parasitic mode excitation.

Compared to full-wave PIC simulations, the developed model retains a significant gain of simulation speed and it still allows a detailed investigation and separation of the involved physical effects.

In contrast to the previous mentioned tools for the simulation of gyro-devices, "SimpleRick" allows the simulation of devices with helically corrugated interaction regions. Such interaction regions are used for so called helical gyrotron traveling-wave tubes (helical gyro-TWTs). This type of vacuum tubes provides a series of advantages compared to classical gyro-TWTs based on cylindrical interaction circuits. The helical gyro-TWTs provide a broader bandwidth and can operate at lower magnetic fields because the electron-wave interaction takes place at the 2nd cyclotron harmonic. In Fig. 1.6.2, simulations of a W-Band helical gyro-TWT developed by the University of Strathclyde are shown. These simulations are performed as a verification of the newly developed interaction code.

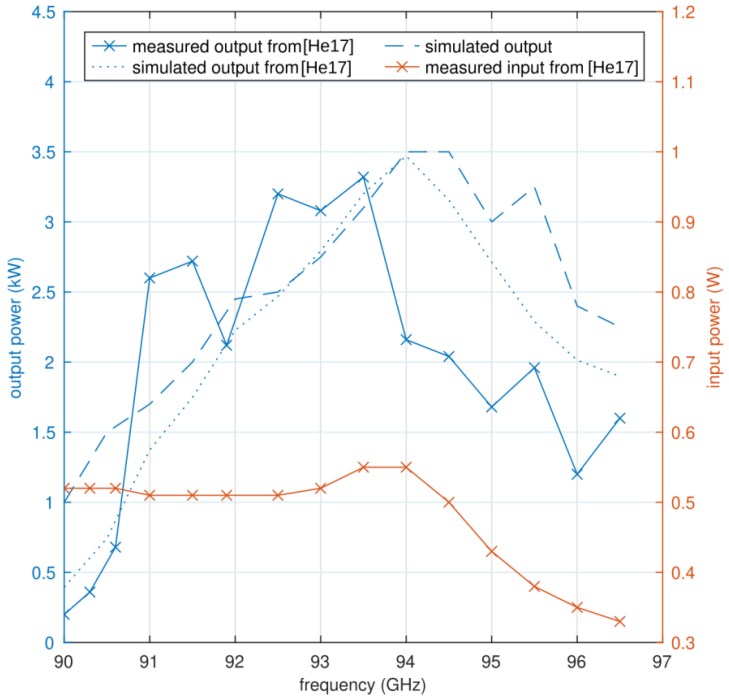

Fig. 1.6.2: Simulated and measured output power of the W-band helical gyro-TWT at different frequencies. For a comparison, also simulated data are shown.

1.7 Generation of ultra-short pulses with new gyro-devices

Contact: M.Sc. Alexander Marek

Systems which are capable to generate ultra-short, coherent pulses in the sub-THz frequency range with a reasonable output power of more than a few Watts are gaining fundamental interest in the research community. The need for new powerful pulsed sources of millimeter and sub-millimeter (sub-THz) radiation is motivated by a large number of fundamental problems and practical applications, as diagnostics of plasma, photochemistry, biophysics, new locating systems, and the spectroscopy of various media. In all cases, novel powerful sub-THz sources of ultra-short coherent pulses would enable the scientific community to develop new devices with improved sensitivity, resolution and data acquisition speed. While coherent pulsed lasers are available since the 1960s, no comparable source of ultra-short coherent pulses at sub-THz frequencies is available up to now.

A solution could be found in a new type of pulsed sub-THz source, utilizing the method of passive mode locking, proposed in 2015 from the Institute of Applied Physics (IAP-RAS) in Nizhny Novgorod and studied in a joint RSF-DFG project from the IHM and the IAP-RAS. The principle of passive mode locking, well known from laser physics, allows the generation of a periodic series of powerful, coherent, ultra-short pulses. A realization for millimeter and sub-millimeter waves consists of an amplifier and a saturable absorber coupled in a feedback loop. The amplifier fulfills the task of the power source and the saturable absorber has a shortening effect on pulses circulating in the feedback loop. While low power signals are strongly attenuated in the saturable absorber, high power signals can pass the absorber with almost no attenuation. Therefore, the low power slopes of a pulse are strongly attenuated while a pulse's high-power peak is not attenuated. This leads to an effective shortening of the pulse and the creation of ultra-short pulses in the feedback loop.

For the generation of powerful, sub-ns pulses at sub-THz frequencies, the active devices, namely the amplifier and absorber, must fulfill challenging properties. Particularly challenging is the demand for a high bandwidth at high power. A promising technology for the amplifier as well as the absorber is the gyrotron traveling-wave tube (gyro-TWT) with helical interaction region. This type of vacuum tube provides a series of advantages compared to classical gyro-TWTs based on cylindrical interaction circuits with dielectric losses. The helical gyro-TWTs provide a higher bandwidth and can operate at lower magnetic fields because the electron-wave interaction takes place at the 2^{nd} cyclotron harmonic. This is of particular interest for the development of devices in the sub-THz range, where the required magnetic field strength for operation at the fundamental cyclotron harmonic can easily exceed 10 T.

As the amplifier and saturable absorber can only be realized in two separate gyro-TWTs, a flexible feedback system based on oversized waveguide components for the coupling of two helical gyro-TWTs to a passive mode locked pulsed oscillator at 263 GHz is developed. The developed feedback system enables a wide range of possible operation regimes of two coupled helical gyro-TWTs. Besides the original purpose as a passive mode-locked pulsed oscillator, the developed feedback system allows the realization of a two-stage amplifier (see Fig. 1.7.1) and the possibility of operating as a frequency tunable, phase-locked backward wave oscillator. These new possibilities could make such a system of coupled helical gyro-TWTs an even more interesting, new high-power RF source for future spectroscopy applications.

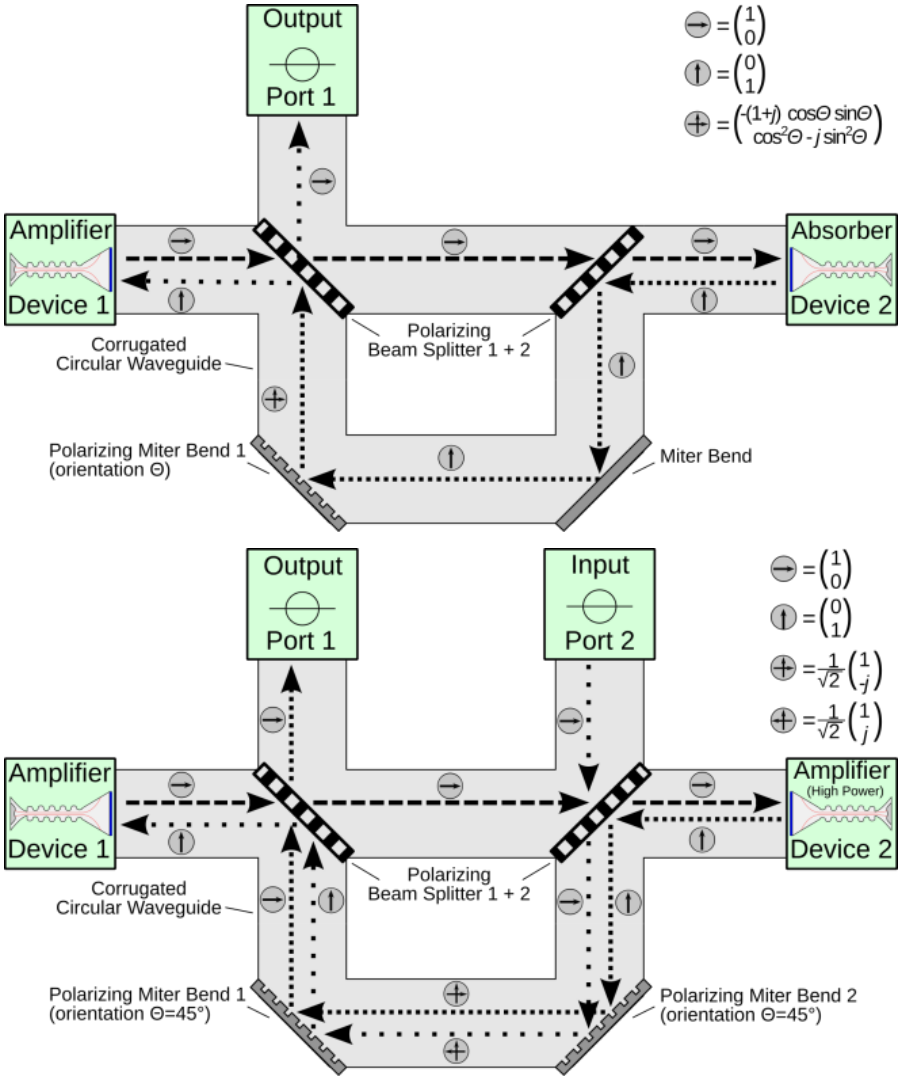

Fig. 1.7.1: Amplifier and absorber devices working with single input-output window coupled by corrugated, overmoded waveguides. The arrows symbolize the polarization of the HE11 mode. Top: Feedback system for a passive mode-locked oscillator; Bottom: Extended design with an addition output/input port and a second polarizing miter bend. The extended design allows e.g. the shown operation of the coupled devices as a two-stage amplifier.

1.8 FULGOR (Fusion Long-Pulse Gyrotron Laboratory)

Contact: Dr. Gerd Gantenbein

The existing gyrotron test facility at KIT, which had been designed and built about 35 years ago, plays a worldwide leading role in the development of high-power gyrotrons for nuclear fusion applications. This facility offered the unique opportunity to develop and test the first CW high power series gyrotrons for the stellarator W7-X in collaboration with IPP and Thales Electron Devices as the industrial partner.

The target parameters of the new gyrotron test facility are well beyond the capabilities of the existing one. The new teststand will strongly support KIT's leading role in the development of advanced gyrotrons. It will help to answer the questions regarding the technical limits and new physical designs for future high-power microwave tubes. The key parameters of FULGOR will be:

- Full CW operation with up to 10 MW electrical power (, corresponding to >= 4 MW RF power (assuming an efficiency of the gyrotron >= 40 %)
- Support of advanced energy recovery concepts, e.g. multi-stage depressed collector (MSDC)

The high voltage power supply (HVPS) will support an operating voltage of up to 130 kV with up to 120 A beam current in short-pulse operation and 90 kV / 120 A in continues wave regime. A superconducting magnet which allows operation of gyrotrons at frequencies well above 200 GHz will be a major component of FULGOR. Other significant components of the teststand are: cooling system, control electronics and interlock system, RF diagnostics including high-power RF absorber loads.

The capabilities of FULGOR will enable the development and CW tests of gyrotrons for future fusion machines like ITER and DEMO. Fig. 1.8.1 is a simplified CAD view of the complete FULGOR system and the status of installation.

Substantial progress has been achieved in the field of diagnostics and procurement of the superconducting magnet. This is a very challenging component since the requirements are beyond what is industrial standard. In 2020 the assembling of the magnet was already finalized at the premise of the manufacturer, TESLA Ltd., GB, first tests of the system are scheduled for Q1/2021.

The body power supply has been ordered at Ampegon PE, Switzerland, delivery and acceptance tests are foreseen at Q2/2021.

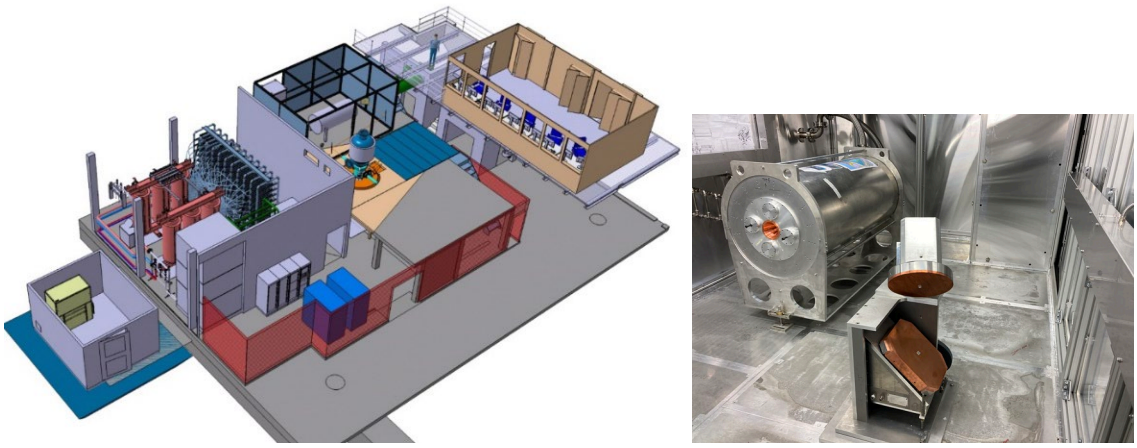

Fig. 1.8.1: CAD view of FULGOR teststand and microwave box with transmission system and RF dummy load.

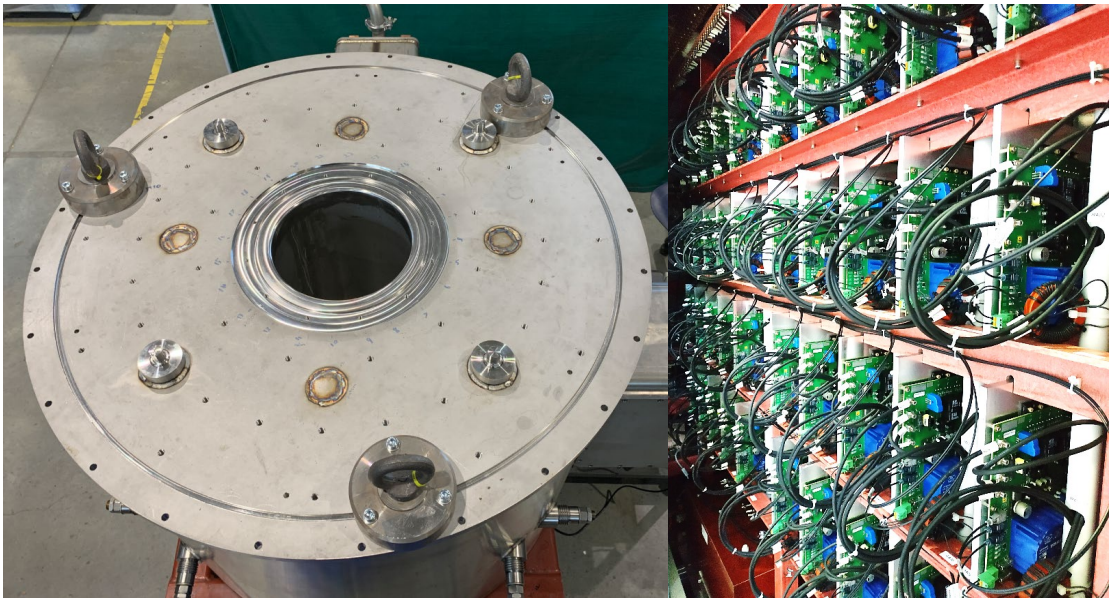

Fig. 1.8.2: Top plate of the 10.5 T magnet and electronic modules of the body power supply.

Involved Staff:

KIT/IHM: D. Albert, Dr. K. Avramidis, B. Ell, **Dr. G. Gantenbein, Dr. S. Illy**, Dr. Z. Ioannidis, Prof. J. Jelonnek, Dr. J. Jin, Th. Kobarg, L. Krier , R. Lang, W. Leonhardt, A. Marek, G. Marschall, D. Mellein, A. Meier (KIT, IAM-AWP), Dr. I. Pagonakis, A. Papenfuß, T. Ruess, **Dr. T. Rzesnicki**, Prof. Dr. T. A. Scherer (KIT, IAM-AWP), M. Schmid, Dr. S. Stanculovic, Dr. D. Strauss (KIT, IAW-AWP), Prof. M. Thumm, J. Weggen, N. Wirth, Dr. Ch. Wu, **IGVP (University of Stuttgart): Dr. C. Lechte**, R. Munk, Dr. B. Plaum, B. Roth, A. Zeitler, **IPP (Greifswald/Garching):** Dr. H. Braune, F. Hollmann, **Dr. H. Laqua**, Dr. S. Marsen, F. Noke, F. Purps, T. Schulz, Dr. T. Stange, P. Uhren

Journal Publications

W7-X Team; Strumberger, E.; Günter, S.; Gantenbein, G.; Huber, M.; Illy, S.; Jelonnek, J.; Kobarg, T.; Lang, R.; Leonhardt, W.; Mellein, D.; Papenfuß, D.; Scherer, T.; Thumm, M.; Wadle, S.; Weggen, J. (2020). Linear, resistive stability studies for Wendelstein 7-X-type equilibria with external current drive. Nuclear fusion, 60 (10), Article no: 106013.

Ioannidis, Z. C.; Chelis, I.; Gantenbein, G.; Rzesnicki, T.; Jelonnek, J. (2020). Experimental Classification and Enhanced Suppression of Parasitic Oscillations in Gyrotron Beam Tunnels. IEEE transactions on electron devices, 67 (12), 5783–5789.

Marek, A.; Avramidis, K.; Ginzburg, N.; Illy, S.; Jelonnek, J.; Jin, J.; Thumm, M. (2020). Extended Feedback System for Coupled Sub-THz Gyro-Devices to Provide New Regimes of Operation. IEEE transactions on electron devices, 67 (12), 5729–5735.

Adya, S.; Yuvaraj, S.; Karmakar, S.; Kartikeyan, M. V.; Thumm, M. K. (2020). Investigations on W-Band Second Harmonic Gyrotron for 50/100-kW Operation. IEEE transactions on plasma science, 48 (12), 4127–4133.

W7-X Team; Liu, S. C.; Liang, Y.; Wang, H. Q.; Killer, C.; Drews, P.; Knieps, A.; Han, X.; Grulke, O.; Krämer-Flecken, A.; Xu, G. S.; Yan, N.; Höschen, D.; Nicolai, D.; Satheeswaran, G.; Geiger, J.; Henkel, M.; Huang, Z.; König, R.; Li, Y.; Neubauer, O.; Rahbarnia, K.; Sandri, N.; Schweer, B.; Wang, E. H.; Wang, Y. M.; Xu, S.; Gao, X.; Gantenbein, G.; Huber, M.; Illy, S.; Jelonnek, J.; Kobarg, T.; Lang, R.; Leonhardt, W.; Mellein, D.; Papenfuß, D.; Scherer, T.; Thumm, M.; Wadle, S.; Weggen, J. (2020). Statistical characteristics of the SOL turbulence in the first divertor plasma operation of W7-X using a reciprocating probe. Physics of plasmas, 27 (12), Article: 122504.

W7-X Team; Wang, Z.; Boscary, J.; Schauer, F.; Gantenbein, G.; Huber, M.; Illy, S.; Jelonnek, J.; Kobarg, T.; Lang, R.; Leonhardt, W.; Mellein, D.; Papenfuß, D.; Scherer, T.; Thumm, M.; Wadle, S.; Weggen, J. (2020). Thermal and mechanical analyses of W7-X plasma facing components for operation phase 2. Fusion engineering and design, 161, Article: 111882.

W7-X Team; Krier, L.; Pagonakis, I. G.; Avramidis, K. A.; Gantenbein, G.; Illy, S.; Jelonnek, J.; Jin, J.; Laqua, H. P.; Marek, A.; Moseev, D.; Thumm, M. (2020). Theoretical investigation on possible operation of a 140 GHz 1 MW gyrotron at 175 GHz for CTS plasma diagnostics at W7-X. Physics of plasmas, 27 (11), Art.-Nr.: 113107.

W7-X Team; Wegner, T.; Alcuson, J. A.; Geiger, B.; von Stechow, A.; Xanthopoulos, P.; Angioni, C.; Beurskens, M. N. A.; Böttger, L.; Bozhenkov, S. A.; Brunner, K. J.; Burhenn, R.; Buttenschön, B.; Damm, H.; Edlund, E. M.; Ford, O. P.; Fuchert, G.; Grulke, O.; Huang, Z.; Knauer, J. P.; Kunkel, F.; Langenberg, A.; Pablant, N. A.; Pasch, E.; Rahbarnia, K.; Schilling, J.; Thomsen, H.; Vano, L.; Gantenbein, G.; Huber, M.; Illy, S.; Jelonnek, J.; Kobarg, T.; Lang, R.; Leonhardt, W.; Mellein, D.; Papenfuß, D.; Scherer, T.; Thumm, M.; Wadle, S.; Weggen, J. (2020). Impact of the temperature ratio on turbulent impurity transport in Wendelstein 7-X. Nuclear fusion, 60 (12).

Wu, C.; Pagonakis, I. G.; Illy, S.; Jelonnek, J. (2020). Two-dimensional leapfrog scheme for trajectories of relativistic charged particles in static axisymmetric electric and magnetic field. Journal of computational physics: X, 8, Article no: 100079.

Wagner, D.; Kasparek, W.; Leuterer, F.; Monaco, F.; Ruess, T.; Stober, J.; Thumm, M. (2020). Correction to: “A Compact Two-Frequency Notch Filter for Millimeter Wave Plasma Diagnostics”. Journal of infrared, millimeter, and terahertz waves, 41, 1591–1592.

W7-X Team; Spring, A.; Grahl, M.; Lewerentz, M.; Klug, C.; Dumke, S.; Bluhm, T.; Laqua, H.; Grun, M.; Holtz, A.; Riemann, H.; Gantenbein, G.; Huber, M.; Illy, S.; Jelonnek, J.; Kobarg, T.; Lang, R.; Leonhardt, W.; Mellein, D.; Papenfuß, D.; Scherer, T.; Thumm, M.; Wadle, S.; Weggen, J. (2020). Metadata Framework for Assisting Experimental Planning and Evaluation at Wendelstein 7-X. IEEE transactions on plasma science, 48 (6), 1409–1414.

W7-X Team; Zanini, M.; Laqua, H. P.; Thomsen, H.; Stange, T.; Brandt, C.; Braune, H.; Brunner, K. J.; Fuchert, G.; Hirsch, M.; Knauer, J.; Höfel, U.; Marsen, S.; Pasch, E.; Rahbarnia, K.; Schilling, J.; Turkin, Y.; Wolf, R. C.; Zocco, A.; Gantenbein, G.; Huber, M.; Illy, S.; Jelonnek, J.; Kobarg, T.; Lang, R.; Leonhardt, W.; Mellein, D.; Papenfuß, D.; Scherer, T.; Thumm, M.; Wadle, S.; Weggen, J. (2020). ECCD-induced sawtooth crashes at W7-X. Nuclear fusion, 60 (10), Article no: 106021.

Petelin, M.; Thumm, M. (2020). On the Elementary Mechanical Effects of the Space-Time-Symmetry Relativity. Natural science, 12 (09), 661–665.

W7-X Team; Slaby, C.; Äkäslompolo, S.; Borchardt, M.; Geiger, J.; Kleiber, R.; Könies, A.; Bozhenkov, S.; Brandt, C.; Dinklage, A.; Dreval, M.; Ford, O.; Fuchert, G.; Hartmann, D.; Hirsch, M.; Höfel, U.; Huang, Z.; McNeely, P.; Pablant, N.; Rahbarnia, K.; Rust, N.; Schilling, J.; von Stechow, A.; Thomsen, H.; Gantenbein, G.; Huber, M.; Illy, S.; Jelonnek, J.; Kobarg, T.; Lang, R.; Leonhardt, W.; Mellein, D.; Papenfuß, D.; Scherer, T.; Thumm, M.; Wadle, S.; Weggen, J. (2020). Investigation of mode activity in NBI-heated experiments of Wendelstein 7-X. Nuclear fusion, 60 (11), 112004.

W7-X Team; Wegner, T.; Geiger, B.; Foest, R.; Jansen van Vuuren, A.; Winters, V. R.; Biedermann, C.; Burhenn, R.; Buttenschön, B.; Cseh, G.; Joda, I.; Kocsis, G.; Kunkel, F.; Quade, A.; Schäfer, J.; Schmitz, O.; Szepesi, T.; Gantenbein, G.; Huber, M.; Illy, S.; Jelonnek, J.; Kobarg, T.; Lang, R.; Leonhardt, W.; Mellein, D.; Papenfuß, D.; Scherer, T.; Thumm, M.; Wadle, S.; Weggen, J. (2020). Preparation, analysis, and application of coated glass targets for the Wendelstein 7-X laser blow-off system. Review of scientific instruments, 91 (8), 083503.

Wagner, D. H.; Kasparek, W.; Leuterer, F. S. P.; Monaco, F.; Ruess, T.; Stober, J. K.; Thumm, M. (2020). A Compact Two-Frequency Notch Filter for Millimeter Wave Plasma Diagnostics. Journal of infrared, millimeter, and terahertz waves, 41 (7), 741–749.

W7-X Team; Knieps, A.; Liang, Y.; Drews, P.; Endler, M.; Grulke, O.; Huang, Z.; Killer, C.; Liu, S.; Nicolai, D.; Rahbarnia, K.; Sandri, N.; Satheeswaran, G.; Gantenbein, G.; Huber, M.; Illy, S.; Jelonnek, J.; Kobarg, T.; Lang, R.; Leonhardt, W.; Losert, M.; Mellein, D.; Papenfuß, D.; Scherer, T.; Thumm, M.; Wadle, S.; Weggen, J. (2020). Design and characteristics of a low-frequency magnetic probe for magnetic profile measurements at Wendelstein 7-X. Review of scientific instruments, 91 (7), 073506.

Ioannidis, Z. C.; Savaidis, S. P.; Mitilineos, S. A.; Livieratos, S.; Stathopoulos, N. A. (2020). Design of Microwave Pulse Compressors Using Small Form-Factor Waveguide Cavities. IEEE transactions on microwave theory and techniques.

W7-X Team; Killer, C.; Shanahan, B.; Grulke, O.; Endler, M.; Hammond, K.; Rudischhauser, L.; Gantenbein, G.; Huber, M.; Illy, S.; Jelonnek, J.; Kobarg, T.; Lang, R.; Leonhardt, W.; Losert, M.; Mellein, D.; Papenfuß, D.;

Scherer, T.; Thumm, M.; Wadle, S.; Weggen, J. (2020). Plasma filaments in the scrape-off layer of Wendelstein 7-X. Plasma physics and controlled fusion, 62 (8), 085003.

W7-X Team; Yu, Q.; Strumberger, E.; Igochine, V.; Lackner, K.; Laqua, H. P.; Zanini, M.; Braune, H.; Hirsch, M.; Höfel, U.; Marsen, S.; Stange, T.; Wolf, R. C.; Günter, S.; Gantenbein, G.; Huber, M.; Illy, S.; Jelonnek, J.; Kobarg, T.; Lang, R.; Leonhardt, W.; Mellein, D.; Papenfuß, D.; Scherer, T.; Thumm, M.; Wadle, S.; Weggen, J. (2020). Numerical modeling of the electron temperature crashes observed in Wendelstein 7-X stellarator experiments. Nuclear fusion, 60 (7), 076024.

W7-X Team; Rudischhauser, L.; Endler, M.; Höfel, U.; Hammond, K. C.; Kallmeyer, J. P.; Blackwell, B. D.; Gantenbein, G.; Huber, M.; Illy, S.; Jelonnek, J.; Kobarg, T.; Lang, R.; Leonhardt, W.; Mellein, D.; Papenfuß, D.; Scherer, T.; Thumm, M.; Wadle, S.; Weggen, J. (2020). The Langmuir probe system in the Wendelstein 7-X test divertor. Review of scientific instruments, 91 (6), 063505.

W7-X Team; Dhard, C. P.; Äkäslompolo, S.; Balden, M.; Baldzuhn, J.; Biedermann, C.; Bräuer, T.; Brezinsek, S.; Endler, M.; Hayashi, Y.; Hwangbo, D.; Kajita, S.; Krause, M.; Kornejew, P.; Masuzaki, S.; Mayer, M.; Motojima, G.; Naujoks, D.; Otte, M.; Rohde, V.; Gantenbein, G.; Huber, M.; Illy, S.; Jelonnek, J.; Kobarg, T.; Lang, R.; Leonhardt, W.; Mellein, D.; Papenfuß, D.; Scherer, T.; Thumm, M.; Wadle, S.; Weggen, J. (2020). Inspection of W 7-X plasma-facing components after the operation phase OP1.2b: observations and first assessments. Physica scripta, 2020 (T171), 014033.

W7-X Team; Wang, E.; Brezinsek, S.; Sereda, S.; Buttenschön, B.; Barbui, T.; Dhard, C. P.; Endler, M.; Ford, O.; Flom, E.; Hammond, K. C.; Jakubowski, M.; Krychowiak, M.; Kornejew, P.; König, R.; Liang, Y.; Mayer, M.; Naujoks, D.; Neubauer, O.; Oelmann, J.; Rasinski, M.; Winters, V. R.; Goriaev, A.; Wauters, T.; Wei, Y.; Zhang, D.; Baumann, K.; Gantenbein, G.; Huber, M.; Illy, S.; Jelonnek, J.; Kobarg, T.; Lang, R.; Leonhardt, W.; Mellein, D.; Papenfuß, D.; Scherer, T.; Thumm, M.; Wadle, S.; Weggen, J. (2020). Impurity sources and fluxes in W7-X: from the plasma-facing components to the edge layer. Physica scripta, 2020 (T171), 014040.

W7-X Team; Niemann, H.; Drewelow, P.; Jakubowski, M. W.; Puig Sitjes, A.; Cannas, B.; Gao, Y.; Pisano, F.; König, R.; Burhenn, R.; Hacker, P.; Reimold, F.; Zhang, D.; Brunner, K. J.; Knauer, J.; Sunn Pedersen, T.; Gantenbein, G.; Huber, M.; Illy, S.; Jelonnek, J.; Kobarg, T.; Lang, R.; Leonhardt, W.; Mellein, D.; Papenfuß, D.; Scherer, T.; Thumm, M.; Wadle, S.; Weggen, J.; Reimold, F.; Zhang, D.; Brunner, K. J.; Knauer, J.; Sunn Pedersen, T. (2020). Large wetted areas of divertor power loads at Wendelstein 7-X. Nuclear fusion, 60 (8), 084003.

Shcherbinin, V. I.; Moskvitina, Y. K.; Avramidis, K. A.; Jelonnek, J. (2020). Improved Mode Selection in Coaxial Cavities for Subterahertz Second-Harmonic Gyrotrons. IEEE transactions on electron devices, 67 (7), 2933–2939.

W7-X Team; Moseev, D.; Laqua, H. P.; Stange, T.; Abramovic, I.; Nielsen, S. K.; Äkäslompolo, S.; Avramidis, K. A.; Braune, H.; Gantenbein, G.; Illy, S.; Jelonnek, J.; Jin, J.; Kasparek, W.; Krier, L.; Korsholm, S. B.; Lechte, C.; Marek, A.; Marsen, S.; Nishiura, M.; Pagonakis, I.; Salewski, M.; Rasmussen, J. J.; Tancetti, A.; Thumm, M.; Wolf, R. C. (2020). Collective Thomson Scattering Diagnostic for Wendelstein 7-X at 175 GHz. Journal of Instrumentation, 15, C05035.

Girka, I. O.; Girka, O. I.; Thumm, M. (2020). Azimuthal surface waves in cylindrical metal waveguides partially filled by magnetoactive plasma: Analysis of energy transfer. Physics of plasmas, 27 (6), 062108.

W7-X Team; Langenberg, A.; Wegner, T.; Pablant, N. A.; Marchuk, O.; Geiger, B.; Tamura, N.; Bussiahn, R.; Kubkowska, M.; Mollén, A.; Traverso, P.; Smith, H. M.; Fuchert, G.; Bozhenkov, S.; Damm, H.; Pasch, E.; Brunner, K.-J.; Knauer, J.; Beurskens, M.; Burhenn, R.; Wolf, R. C.; Gantenbein, G.; Huber, M.; Illy, S.; Jelonnek, J.; Kobarg, T.; Lang, R.; Leonhardt, W.; Mellein, D.; Papenfuß, D.; Scherer, T.; Thumm, M.; Wadle, S.; Weggen, J. (2020). Charge-state independent anomalous transport for a wide range of different impurity species observed at Wendelstein 7-X. Physics of plasmas, 27 (5), 052510.

Thumm, M. (2020). Gyro-devices – natural sources of high-power high-order angular momentum millimeter-wave beams. Terahertz Science & Technology, 13 (1), 1–21.

Savaidis, S. P.; Mitilineos, S. A.; Ioannidis, Z. C.; Stathopoulos, N. A. (2020). Experiments on the Pulse Repetition Frequency Optimization of 1.3-GHz, 100-kW Microwave Pulse Compressor. IEEE transactions on microwave theory and techniques, 68 (6), 2374–2381.

W7-X Team; Baldzuhn, J.; Damm, H.; Beidler, C. D.; McCarthy, K.; Panadero, N.; Biedermann, C.; Bozhenkov, S. A.; Dinklage, A.; Brunner, K. J.; Fuchert, G.; Kazakov, Y.; Beurskens, M.; Dibon, M.; Geiger, J.; Grulke, O.; Höfel, U.; Klinger, T.; Köchl, F.; Knauer, J.; Kocsis, G.; Kornejew, P.; Lang, P. T.; Langenberg, A.; Laqua, H.; Pablant, N. A.; Pasch, E.; Pedersen, T. S.; Ploeckl, B.; Rahbarnia, K.; Schlisio, G.; Scott, E. R.; Stange, T.; Von Stechow, A.; Szepesi, T.; Turkin, Y.; Wagner, F.; Winters, V.; Wurden, G.; Zhang, D.; Gantenbein, G.; Huber, M.; Illy, S.; Jelonnek, J.; Kobarg, T.; Lang, R.; Leonhardt, W.; Mellein, D.; Papenfuß, D.; Scherer, T.; Thumm, M.; Wadle, S.; Weggen, J. (2020). Enhanced energy confinement after series of pellets in Wendelstein 7-X. Plasma physics and controlled fusion, 62 (5), 055012.

W7-X Team; Kremeyer, T.; Flesch, K.; Schmitz, O.; Schlisio, G.; Wenzel, U.; Gantenbein, G.; Huber, M.; Illy, S.; Jelonnek, J.; Kobarg, T.; Lang, R.; Leonhardt, W.; Mellein, D.; Papenfuß, D.; Scherer, T.; Thumm, M.; Wadle, S.; Weggen, J. (2020). Wisconsin In Situ Penning (WISP) gauge: A versatile neutral pressure gauge to measure partial pressures in strong magnetic fields. Review of scientific instruments, 91 (4), 043504.

W7-X Team; Krämer-Flecken, A.; Han, X.; Otte, M.; Anda, G.; Bozhenkov, S. A.; Dunai, D.; Fuchert, G.; Geiger, J.; Grulke, O.; Pasch, E.; Scott, E. R.; Trier, E.; Vécsei, M.; Windisch, T.; Zoletnik, S.; Gantenbein, G.; Jelonnek, J.; Thumm, M. (2020). Investigation of turbulence rotation in the SOL and plasma edge of W7-X for different magnetic configurations. Plasma science & technology, 22 (6), 064004.

W7-X Team; Perseo, V.; Gradic, D.; König, R.; Ford, O. P.; Killer, C.; Grulke, O.; Ennis, D. A.; Gantenbein, G.; Huber, M.; Illy, S.; Jelonnek, J.; Kobarg, T.; Lang, R.; Leonhardt, W.; Mellein, D.; Papenfuß, D.; Scherer, T.; Thumm, M.; Wadle, S.; Weggen, J. (2020). Coherence imaging spectroscopy at Wendelstein 7-X for impurity flow measurements. Review of scientific instruments, 91 (1), Article: 013501.

W7-X Team; Ford, O. P.; Vanó, L.; Alonso, J. A.; Baldzuhn, J.; Beurskens, M. N. A.; Biedermann, C.; Bozhenkov, S. A.; Fuchert, G.; Geiger, B.; Hartmann, D.; Jaspers, R. J. E.; Kappatou, A.; Langenberg, A.; Lazerson, S. A.; McDermott, R. M.; McNeely, P.; Neelis, T. W. C.; Pablant, N. A.; Pasch, E.; Rust, N.; Schroeder, R.; Scott, E. R.; Smith, H. M.; Wegner, T.; Kunkel, F.; Wolf, R. C.; Gantenbein, G.; Huber, M.; Illy, S.; Jelonnek, J.; Kobarg, T.; Lang, R.; Leonhardt, W.; Mellein, D.; Papenfuß, D.; Scherer, T.; Thumm, M.; Wadle, S.; Weggen, J. (2020). Charge exchange recombination spectroscopy at Wendelstein 7-X. Review of scientific instruments, 91 (2), Article: 023507.

W7-X Team; Lobsien, J.-F.; Drevlak, M.; Jenko, F.; Maurer, M.; Navarro, A. B.; Nührenberg, C.; Pedersen, T. S.; Smith, H. M.; Turkin, Y.; Gantenbein, G.; Huber, M.; Illy, S.; Jelonnek, J.; Kobarg, T.; Lang, R.; Leonhardt, W.; Mellein, D.; Papenfuß, D.; Scherer, T.; Thumm, M.; Wadle, S.; Weggen, J. (2020). Physics analysis of results of stochastic and classic stellarator coil optimization. Nuclear fusion, 60 (4), Article: 046012.

Girka, I. O.; Pavlenko, I. V.; Thumm, M. (2020). Rotation of electromagnetic energy initiated by azimuthal surface waves in coaxial metal waveguides entirely filled by plasma. Physics of plasmas, 27 (3), 032104.

W7-X Team; Fuchert, G.; Brunner, K. J.; Rahbarnia, K.; Stange, T.; Zhang, D.; Baldzuhn, J.; Bozhenkov, S. A.; Beidler, C. D.; Beurskens, M. N. A.; Brezinsek, S.; Burhenn, R.; Damm, H.; Dinklage, A.; Feng, Y.; Hacker, P.; Hirsch, M.; Kazakov, Y.; Knauer, J.; Langenberg, A.; Laqua, H. P.; Lazerson, S.; Pablant, N. A.; Pasch, E.; Reimold, F.; Sunn Pedersen, T.; Scott, E. R.; Warmer, F.; Winters, V. R.; Wolf, R. C.; Gantenbein, G.; Huber, M.; Illy, S.; Jelonnek, J.; Kobarg, T.; Lang, R.; Leonhardt, W.; Mellein, D.; Papenfuß, D.; Scherer, T.; Thumm, M.; Wadle, S.; Weggen, J. (2020). Increasing the density in Wendelstein 7-X: benefits and limitations. Nuclear fusion, 60 (3), 036020.

Pagonakis, I. G.; Avramidis, K. A.; Gantenbein, G.; Illy, S.; Ioannidis, Z. C.; Jin, J.; Kalaria, P.; Piosczyk, B.; Ruess, S.; Ruess, T.; Rzesnicki, T.; Thumm, M.; Jelonnek, J. (2020). Triode magnetron injection gun for the KIT 2 MW 170 GHz coaxial cavity gyrotron. Physics of plasmas, 27 (2), Article no: 023105.

Thumm, M. (2020). State-of-the-Art of High-Power Gyro-Devices and Free Electron Masers. Journal of infrared, millimeter, and terahertz waves, 41 (1), 1–140.

2 Renewable Energy (RE): Bioenergy -Feedstocks and Pretreatment-

Contact: Prof. Dr. Georg Müller

The Department for Pulsed Power Technology is focusing on research and development of pulsed power technologies and related applications. The applications involves the electroporation of biological cells for extraction of cell contents (PEF- process), dewatering and drying of green biomass, pre-treatment of micro algae for energetic use and sustainable reduction of bacteria in contaminated effluents. Another key research topic is devoted to the development of corrosion barriers and materials for improved compatibility of structural materials in contact with liquid metal coolants. This year's report focuses primarily on the activities and results of ongoing third-party funded projects of the department.

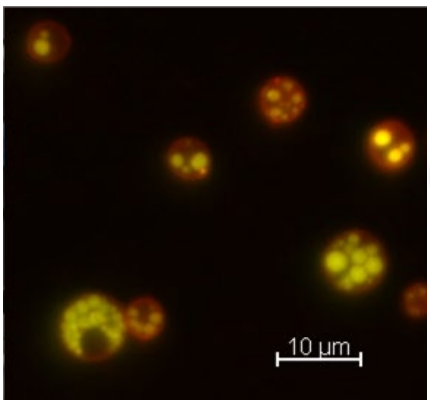

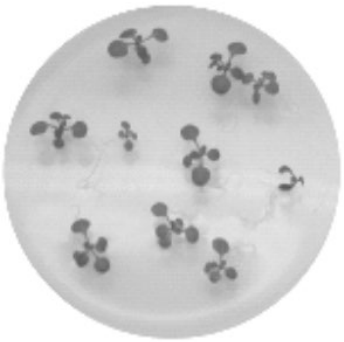

PEF treatment, 10ns pulses

2.1 PEF-processing of microbial biomass and industrial water streams

Contact: Dr. Wolfgang Frey

2.1.1 SABANA-Project: PEF-assisted cascade processing of microalgae

The EU-Project SABANA focusses on products for agriculture and aquaculture produced from microalgae feedstocks. For biofertilizer production, the protein inventory of microalgae is converted into amino-acid concentrates by enzymatic hydrolysis and used for sustainable fertilizing, whereas the lipid inventory can be used as a high value supplement to enrich aquafeed pellets by polyunsaturated fatty acids, essential for high quality fish feeding.

PEF-assisted cascade processing allows efficient recovery of both products sequentially. In order to demonstrate cascade-processing capabilities, lipid extraction was performed on *Scenedesmus* biomass after it was processed by enzymatic hydrolysis (EH). For comparison, the lipid yield from fresh biomass directly after harvesting was determined (Fig. 2.1.1). Lipid extraction performed on untreated fresh biomass enables to recover about one third of the lipid content, more precisely 39 %. This percentage increases to 72 % if fresh biomass was treated by PEF before lipid extraction.

In the case that the biomass went through the process of enzymatic hydrolysis first, lipid yields are identical and very close to the lipid yield obtained immediately after PEF treatment, i.e. 70 %. In contrast, the lipid yield obtained after high pressure homogenization (HPH) and subsequent enzymatic hydrolysis was much lower. Only 50 % of the lipids could be recovered. This decrease of the lipid yield in case of HPH pre-treatment was not investigated in detail but it is suspected that due to emulsion formation during HPH, a part of the lipids was discarded with the water phase.

This comparison of different pretreatment technologies clearly shows the advantage of PEF-assisted cascade processing over HPH pretreatment. The first mentioned allows lipid recovery at about 40 % higher efficiency.

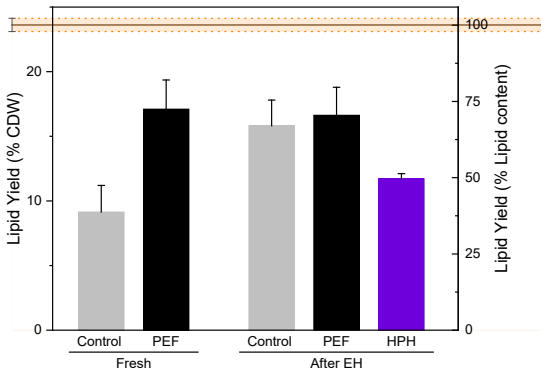

Fig. 2.1.1: Lipid yields after PEF treatment and after enzymatic hydrolysis, EH, of *S. almeriensis*. The results are displayed as a percentage of the cell dry weight, CDW. Results are displayed as average+std of 3 independent experiments. Total lipid content, displayed as a horizontal orange bar (±std), was obtained using the Kochert protocol.

Collaboration: University of Almería, GEA Westfalia, Biorizon

Funding: H2020, SABANA, Grant Agreement No. 727874

2.1.2 DiWaL: PEF-demo facility for PEF-treatment of electrodeposition paints

PEF-treatment was demonstrated to efficiently inactivate bacteria in electrocoating process media. In collaboration with Eisenmann SE for PEF-treatment of electrodeposition paints, EDP, a demonstration facility was built and operated. It consists of a media transport unit, visible to the left behind the control cabinet. It enables a paint transport at a massflow of 0.8 m3/h. The semiconductor generator consists of two towers, each housing 15 fullbridge 1 kV, 0.6 kA generator modules including charging control units providing a nominal pulse output amplitude of 30 kV when erected. On top of the generator towers the treatment chamber section is mounted inside the cabinet.

After some revision steps for improving electromagnetic compatibility of module control and power electronics, continous operation could be accomplished for several hours at increasing workload, but had to be stopped due to unsufficient media cooling capabilities of the heat exchangers in the media transport unit. Further optimization of the media transport unit was not possible since in the meanwhile Eisenmann SE was adjudged insolvent and is currently being capitalized. The project was stopped at that point in September 2020.

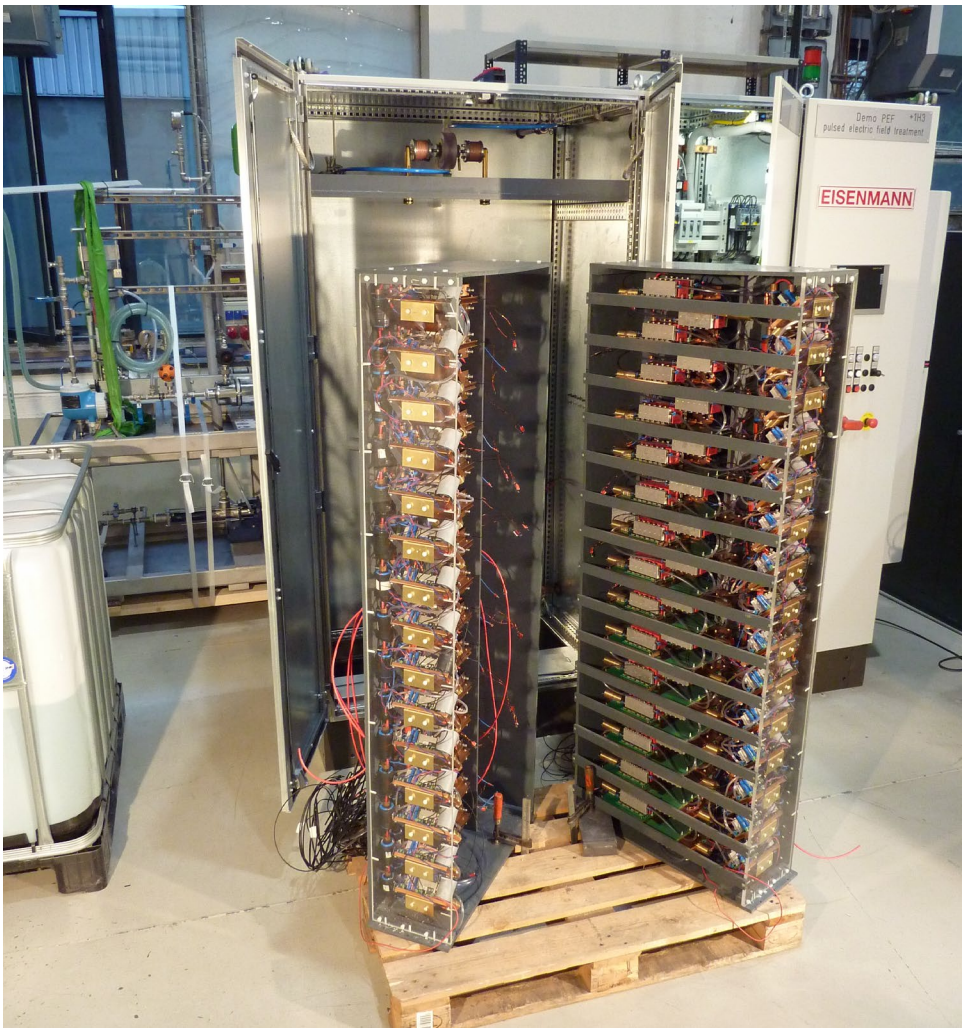

Fig. 2.1.2: PEF-Demo-Facility for bacterial inactivation of electrocoating process media. The facility consists of a 30 stage modular semiconductor-switched pulse generator, front, a control cabinet, middle, and the media transport unit in the rear.

2.1.3 DiWaL: Bacterial decontamination of electro-dip paints by PEF-treatment

In the DiWaL project, the PEF treatment was used for the first time as a purely physical method to reduce the bacterial load in the aqueous electro-dip paints. We have developed a process based on bipolar pulses that reduces bacteria in an energy-efficient manner and at the same time avoids undesired coating of the electrodes of the treatment cell with dip paints. In the course of the work it could be shown that the PEF treatments with pulses of 1.0 µs, regardless of the pulse shape unipolar or bipolar, reduce the bacterial concentration in the cathodic dip coating by more than 2.0 log, with an energy input of less than 40 $kJ \cdot l^{-1}$. The peripheral aqueous streams identified as possible source of bacterial contamination could also be effectively decontaminated using PEF treatment. These results show that PEF technology meets the disinfection requirements that ensure trouble-free operation in electro-dip paint shops.

2.1.4 Anaerobic Digestion (AD) as final step for complete utilization of previously PEF-treated microalgal biomass

Anaerobic digestion of residual microalgal biomass turned out to be a promising final step in complete utilization of microalgal biomass. After extracting all valuable components (proteins, lipids, oligo/polysaccharides, pigments, anti oxidants, etc.), the rest of the remaining organic volatile substances (VS) get not lost and are converted into biogas, and subsequently refined to biomethane, an easy storable and transportable form of energy. The handling of the rest biomass is quite pleasant, as beside the addition of water and the inoculum, i.e. the anaerobic microorganisms, no additives or additional pretreatment before AD is required. The extraction of microalgal valuables, supported by PEF-treatment, was reported earlier (data published in IHM annual report 2019) and the generation of biogas (containing approx. 73-95 % bio methane) was described in a qualitative manner, previously. Hereafter the quantitative specific methane yields from different previously exploited microalgae preparations, obtained by AD, performed with our cooperation partner, the Helmholtz Centre for Environmental Research (UFZ Leipzig), are illustrated.

Contributions of the inoculum to the specific biomethane yield were reproducible, with a final asymptotic approximation of almost 30 mL_{norm}/g_{VS}, which were deducted from the biomethane yields of the individual investigated species.

Within the first week of AD the control sample produced methane faster, at a higher level as the PEF-treated sample. Investigations of untreated control samples (no PEF-treatment) didn´t demonstrate the presence of significant amounts of lipids in the surrounding medium. That´s why it shall be assumed that most probably no, or at least no relevant long chain fatty acid (LCFA)-concentrations are present in the microalgae medium. LCFAs are inhibitors, which adsorb at the anaerobic microorganism´s surface, hampering their metabolism and the AD-process, hence. This would help to explain, why the control sample initially demonstrated no inhibition in AD, comparable to the lipid extracted samples. After overall 11 days, control- and PEF-treated samples converged and showed very similar methane yields until day 28. From this point on both samples showed identical specific methane yields and finished after 38 day at a level of 470 mL_{norm}/g_{VS}. PEF-treated samples with and without aqueous extraction, might experienced a minor release of LCFA´s, causing a visible delay in rise of specific methane yield, in the initial phase of AD (Fig. 2.1.3). The high phosphate and phosphorus-concentrations in the microalgae medium of PEF treated microalgae (data published in IHM annual report 2019), which are immediately available for the anaerobic consortium, could be an additional reason, for the initially delayed methane production. There are hints that phosphate concentrations from 20 mM could inhibit methanogenesis.

Regarding AD, PEF-treated and subsequent lipid extracted samples and the control samples showed comparable, intensive performances, in the first couple of days. Lipid extracted samples reduced their increase of spec. methane yield drastically after 4 days, with only marginal increase of specific methane yield, throughout the remaining 5 wks of AD. Final specific methane yield was 205 mL_{norm}/g_{VS}. No negative impact on AD with lipid extracted biomass was expected, due to the lack of lipids and therefore also the lack of LCFAs. From LCFAs its known that compared to faster hydrolysis, they slow down AD by an alternative, slower breakdown mechanism for fatty acids, the β-oxidation.

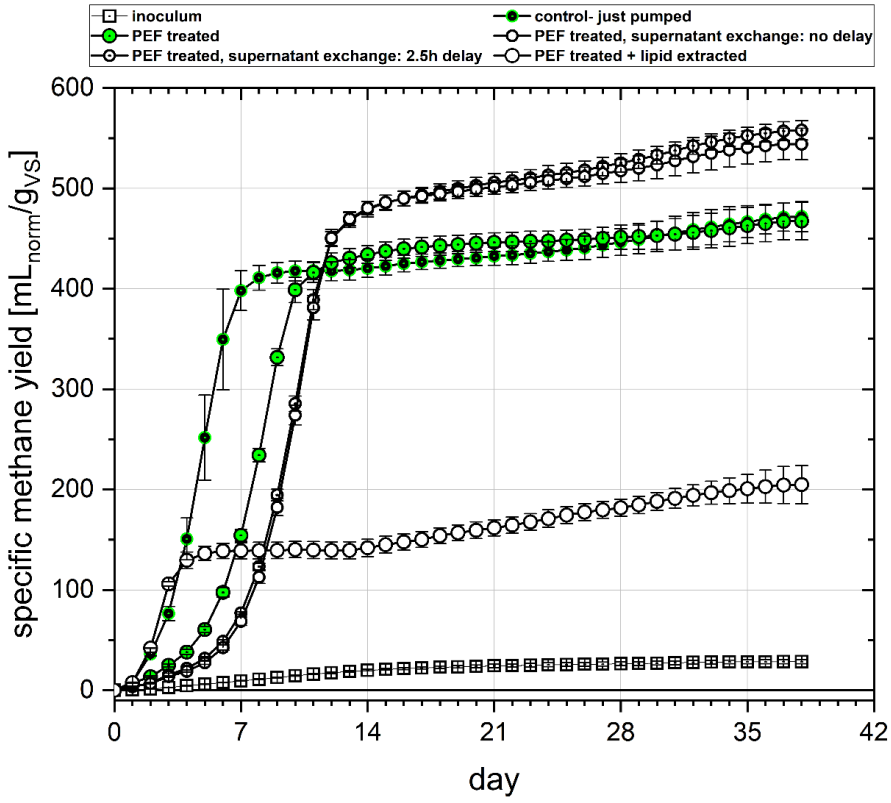

Fig. 2.1.3: Specific methane yields of differently treated preparations of microalgae *A. protothecoides* and contribution of inoculum to specific methane yield.

Directly after PEF-treatment, a selection of samples was subjected to an aqueous extraction, in two ways. The concept was to examine the impact of different extraction periods ($t_{extract}$ = 0 min and $t_{extract}$ = 150 min) and the responding release of different amounts of algal ingredients, on AD. As the aqueous extracted species were removed by centrifugation and replaced by deionized water, after respective extraction periods, a different behavior, during AD was expected. These aqueous extracted samples, demonstrated highest specific methane yields in all conducted experiments, peaking at roughly 550 mL_{norm}/g_{VS} after 38 d of AD. Both aqueous extracted algal biomasses, though at different extraction periods, showed similar, in parts even identical methane yield progression. This suggests there are no significant differences in the composition of the two species with different extraction periods. This assumption was proved by another experiment with aqueous extraction periods from $t_{extract}$ = 0 min - 150 min, performed in 30 min-steps (data not shown).

2.1.5 Lipid recovery from oleogenic yeast

Compared to microalgae lipids, the lipid inventory of most oleogenic yeasts exhibit a higher degree of fatty acid saturation. This makes them suitable for biolubricants applications. First orienting experiments on lipid recovery performed by IHM and BLT2/TEBI were conducted on fresh oleaginous yeast *Saitozyma podzolica* DSM 27192 grown in nitrogen-depleted medium in order to stimulate lipid production.

PEF-treatment was applied and followed by lipid extraction using ethanol and hexane blends. Two approaches were compared. In first approach, the yeast was processed directly after harvesting in their initial cultivation medium and in the second approach, the suspension was slightly washed in order to lower the ion content and therefore match the conductivity that was typically used in the past for microalgae. Lipid yield obtained in the second approach, i.e with the washed suspension, are displayed in Fig. 2.1.4 for different specific energy inputs. The results proved that transposition of protocols developed on microalgae were already efficient on yeast suspension. Indeed, treatments of only 50 kJ/L and 100 kJ/L enabled to extract 87 % and 99 % of the lipid content.

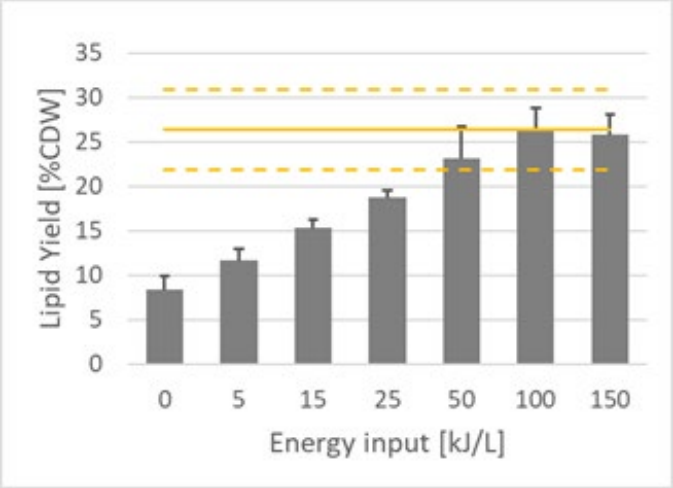

Fig. 2.1.4: Lipid yields obtained by solvent extraction after PEF treatment. The yellow continuous line and the two dashed lines represent the total lipid content of the three cultivations evaluated by using bead-milling and soxhlet extraction and are displayed as average ±std.

Within the frame of this first study, extraction of the lipids required less than 11 MJ/kg_{LIPID} (3 kWh/kg_{LIPID}) at a biomass concentration of 20 g_{dw}/l during PEF-processing. From the energetic aspect, already at this low biomass concentration, our approach very well competes with some of the best reported values for lipid extraction such as hydrochloric acid digestion under heat of *Cryptococcus curvatus* biomass which requires 9.3-18.6 MJ/kgLIPID (2.58-5.17 kWh/kgLIPID) or enzymatic digestion of *Rhodosporidium toruloides* biomass which requires 13.3 MJ/kgLIPID (3.67 kWh/kg_{LIPID}).

Additional improvements for PEF-processing of oleogenic yeasts are expected. In particular, a treatment of suspensions with higher biomass concentration was proven a successful approach for low-energy-demand microalgae processing and will be transferred to yeast processing. In addition, an optimization of PEF-processing parameters to yeast cells has not been performed, yet. Furthermore, the treatment of yeast suspension at higher conductivity i.e. without washing, which was in this study less efficient and required about 3 times more energy, should be further investigated, since this exhibits potential to reduce overall processing costs. Latter will open the research-area of PEF-treatment at high conductivity levels, which will be addressed in detail in future.

2.1.6 Recovery of proteins from *Chlorella vulgaris* using PEF treatment

During this year, we have made an important step forward in our endeavor to achieve the goals of POF III (Research Program on Renewable Energies - Topic 3: Bioenergy, Helmholtz Gemeinschaft) and to establish cascade processing for the valorization of microalgae biomass. With our evaluated treatment methods, we were able to recover up to 50 % of the proteins from Chlorella vulgaris after PEF treatment followed by an additional incubation step. In addition, the specific treatment energy was reduced by a factor of ten (Fig. 2.1.5).

The key point is, that only a part of the microalgae needs to be inactivated, as a death factor is released during the incubation step, which inactivates other algae. We were able to show that water-soluble extracts from PEF-treated microalgae suspensions, which were incubated for 24 h, led to the death of living microalgae, although these recipient cells had not been directly subjected to PEF treatment.

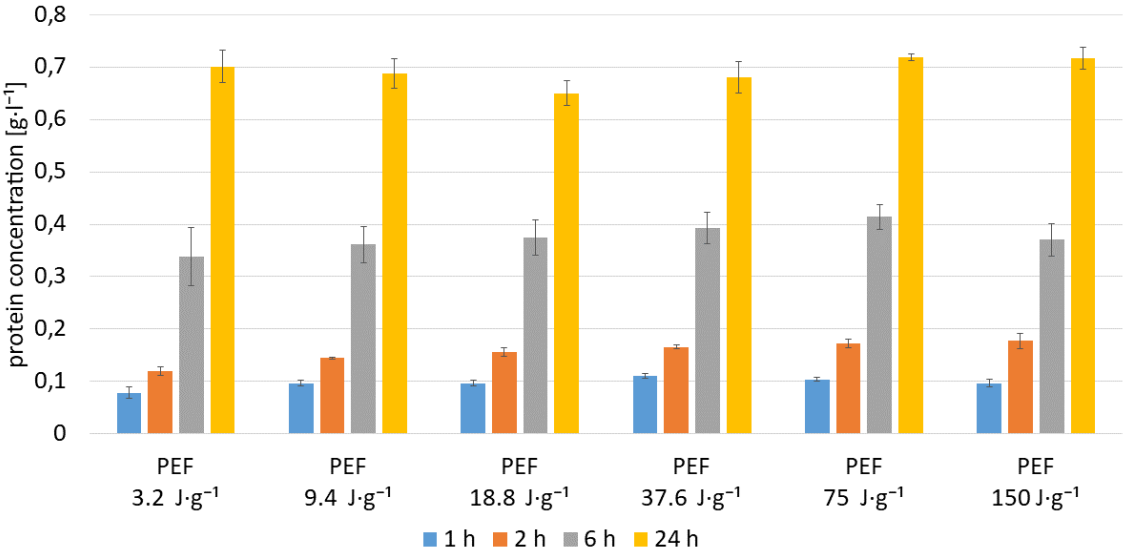

Fig. 2.1.5: Concentration of substances in supernatants from PEF-treated microalgae biomass for different incubation times (delay) after PEF-treatment, for untreated biomass (harvest) and for PEF-treated biomass after lipid extraction, analyzed on day of the experiment, top, and analyzed 20 days after the experiment, bottom.

Our working model proposes that PEF treatment induces programmed cell death in C. vulgaris, while specifically releasing a cell-death inducing factor. Mild PEF treatment including a subsequent incubation period could be a novel biotechnological strategy to extract first water-soluble proteins and subsequently lipids in a cascade process without wasting energy on drying of the biomass or high treatment energies while still providing product safe for consumption.

Collaboration: Botanical Institute

Funding: Research Program on Renewable Energies - Topic 3: Bioenergy, Helmholtz Gemeinschaft

2.2 Components and electroporation processes

Contact: PD Dr. Martin Sack

2.2.1 ZIM-Wine

In the frame of the joint research project "PEF-treatment of crushed grapes (Elektroporation von Traubenmaische)" a device for the treatment of crushed grapes by pulsed electric fields (PEF) with a flow rate of 10 t/h has been developed in collaboration with the industrial partners ARMBRUSTER Keltereitechnologie and KEA-TEC. The project has been supported by the Federal Ministry for Economic Affairs and Energy on the basis of a decision by the German Bundestag. Already during the year 2019 the electroporation device has been put into operation and tested successfully and in 2020 a report about the project results has been furnished.

In autumn 2020 after the end of the project's funding period the operation of the electroporation device has been demonstrated successfully on site at the winemakers' cooperative "Winzer von Baden" in Wiesloch. In the course of two experimental runs, a total amount of 30 t of crushed grapes of the grape variety Pinot Noir has been processed, i.e. 15 t per run. The device has been operated at a flow rate of up to 4.7 m³/h and at an average power of up to 33 kW. The effect of electroporation was well perceptible. Fig. 2.2.1 shows the electroporation device on site at the winery.

Fig. 2.2.1: Electroporation device on site at the winery.

Collaboration: ARMBRUSTER Keltereitechnologie, KEA-TEC

Funding: The project is supported by the Federal Ministry for Economic Affairs and Energy on the basis of a decision by the German Bundestag.

Supported by:
ZIM Zentrales Innovationsprogramm Mittelstand
Federal Ministry for Economic Affairs and Energy
on the basis of a decision by the German Bundestag

2.2.2 Semiconductor-based Marx-type pulse generator for PEF-treatment of potatoes

For the PEF-treatment of potatoes in industrial scale a Marx-type pulse generator equipped with IGBT switches is currently being developed. For an energy-efficient operation of the pulse generator, the pulse switches are operated under soft-switching conditions and resonant charging is applied. The generator has been designed for an operation at a stage voltage of between 50 V and 1 kV. It delivers a peak pulse current of up to 500 A into an RLC pulse circuit with a pulse length in the order of 10 µs. Stacks of 6 and 8 stages have been tested successfully in a ground-symmetric arrangement connected to an artificial resitive load. The generator design involves cooling of the power semiconductors by means of natural convection of air. Fig. 2.2.2 shows the voltages and currents measured at the positive and negative output of the 6-stage arrangement and at the outputs of both ground-side stages. Fig. 2.2.3 shows the voltage across the stages and the charging current during resonant charging. At a peak charging current of approximately 72 A the stage capacitors are re-charged within 900 µs to a voltage of twice of the supply voltage. So far, the generator has been tested successfully in a 6- and 8-stage configuration at a charging voltage of up to 1 kV per stage, a peak pulse current ranging between approximately 400 A and 500 A at corresponding pulse lengths between 10 µs and 15 µs, and a pulse repetition rate of up to 500 Hz. Thereby, an average electric power of up to 8.9 kW has been supplied to the generator. The temperatures of the power semiconductors remained within acceptable limits.

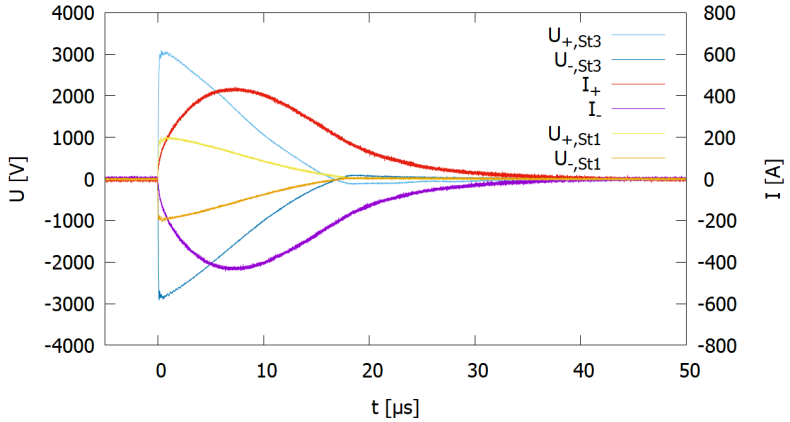

Fig. 2.2.2: Voltages and currents at the genertor's positive and negative output terminal and at the outputs of both ground-side stages.

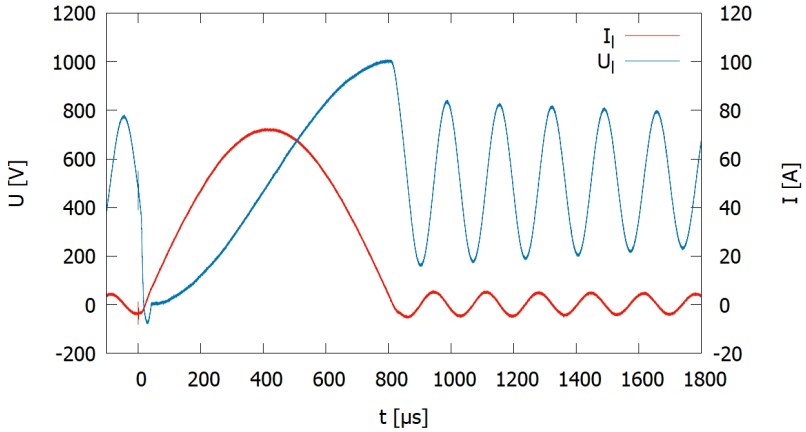

Fig. 2.2.3: Stage voltage and charging current during resonant charging of the generator.

2.3 Concentrating Solar Power (CSP)/ Liquid metal

– Material research – improving the compatibility of materials for CSP

Contact: Dr. Alfons Weisenburger

Liquid metals as advanced heat-transfer media (HTM) and storage media for CSP are a promising research area that will result in performance and efficiency increase and reduced costs. Within LIMCKA (Liquid Metal Competence Center KArlsruhe) several institutes and laboratories of the KIT combine their long-standing experience and specific expertise in material research, system engineering, safety and thermal-hydraulics to tackle all relevant aspects of liquid metals as HTM. The IHM focuses on compatibility research by surface optimization of existing materials using GESA and development of new materials that are able to mitigate corrosion in contact with liquid metals and salts. Liquid metal batteries are a new research area where the expertise of the IHM and DLR is combined with the expertise of a Chinese university (HUST) to explore Sb-Bi(Sn)/ Na based low cost liquid metal battery concepts in the frame of a German-Chinese DFG project. The technical feasibility and scaling of CO_2-free methane pyrolysis in liquid high-temperature Sn (> 1000 °C) is investigated as part of the DECAGAS project together with ITES and WINTERSHALL-DEA.

Some of the tasks are embedded in European projects, the EERA-CSP and cooperations like with DLR and HUST via the DFG or in direct industrial cooperations.

The most relevant results obtained in the reporting period are presented briefly:

2.3.1 GESA – SOFIE

Contact: DP Wladimir An

Based on the Laser-induced fluorescence LIF-Dip diagnostics principle and the use of a wide-band excitation laser, we developed a method that enables the measurements of weak electric fields in plasmas with poor microscale pulse-to-pulse reproducibility. The new measurement technique not only allows the entire Stark spectrum of a point to be recorded in just one measurement process, but also provides the complete image of the one-dimensional electric field distribution, stretched to macroscopic plasma areas of a few cm.

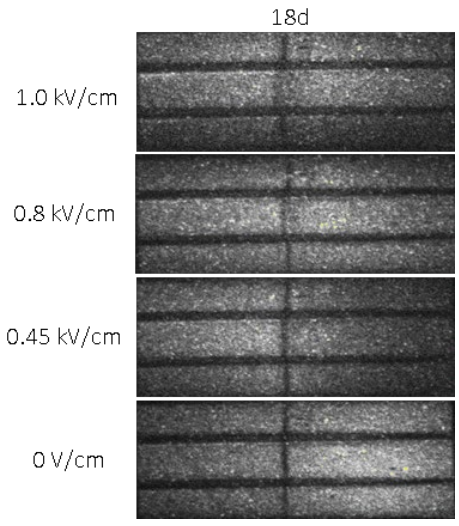

Fig. 2.3.1: Field-Distribution method: Dip shift for 18d[3/2]$_1$ in different electric field.

2.3.2 Material development

Contact: Dr. Alfons Weisenburger

Five Al-Cr-Fe-Ni based high entropy model alloys (HEA) with dominant FCC phase have been designed and prepared. The corrosion tests of as-cast alloys in oxygen-containing molten Pb show their promising corrosion resistances at 600°C, which is due to the formation of protective $(Fe,Cr)_3O_4/Al_2O_3$ or Cr_2O_3/Al_2O_3 bi-layer. Based on the obtained results, three Al-Cr-Fe-Ni-X (X: Cu, Ti or Nb) HEAs have been further designed targeting for improved mechanical properties. The experimental results indicate that the fifth principle elements (Cu, Ti or Nb) not only modify the microstructure of Al-Cr-Fe-Ni model alloy, but also have significant influences on the hardness, corrosion behaviour and microstructure stability (after thermal aging).

Several ceramic materials have shown their capability to be applied as structural material for the CO_2-free methane pyrolysis in liquid Sn at temperatures above 1000°C based on 1000 h tests. Long term tests up to 10,000 h and at temperatures of 1150°C are ongoing for the final examination. First exposure tests of joint ceramics that are required for construction and assembling are performed and show at least one potential joining methode

2.3.3 Liquid metal battery

Contact: M.Sc. Tianru Zhang

A liquid metal battery consists of three different liquids, which stay separated due to density differences and mutual immiscibility. The negative electrode is a low-density liquid metal, in our case sodium, a medium-density molten salt is the electrolyte and the positive electrode is a high-density liquid metal. For the latter Sb-Sn and Sn-Bi alloys are selected.

One issue is the compatibility of the structural materials with the used liquids. In a first step the behaviour of potential structural materials in Sb_3Sn_7 and $SbBi_9$ at temperatures between 370-450 °C up to 750 h were tested in the existing COSTA facility with a reducing atmosphere ($Ar5\%H_2$) above the liquid metal. For exposure tests ten different materials (various steels, elemental Mo and Cr, 3 Max-phase coatings on Al_2O_3 substrate (Ti_2AlC, Ti_3AlC_2, Cr_2AlC)) were chosen. Results showed clearly that the Sb-Sn system is more aggressive than the Sb-Bi system. All steels as well as the elemental Cr showed strong corrosion attack. Only Mo has a good corrosion resistance against the liquid metal. Furthermore, all 3 Max-phases presented promising corrosion resistance.

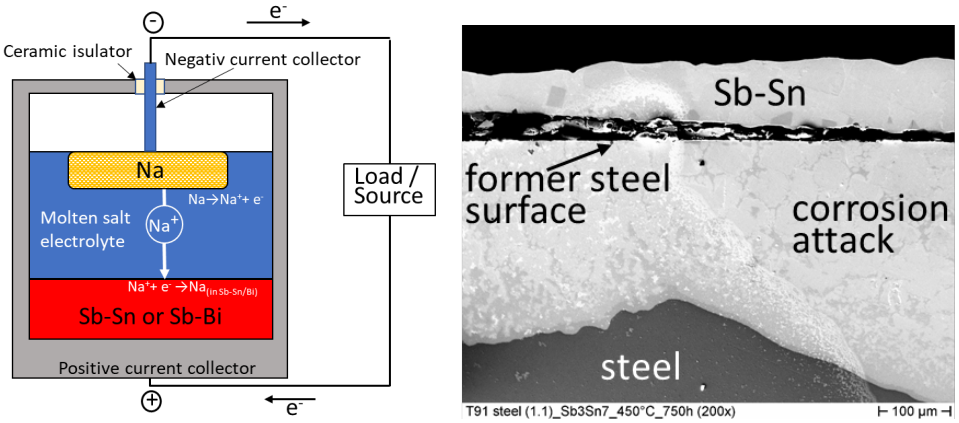

Fig. 2.3.2: Left: Sheme of a liquid metal battery. Right: T91 steel after exposure to Sb3Sn7 at 450 °C for 750 h

Involved Staff:

Dr. S. Akaberi, DP W. An, K. Baumann, Dr. R. Fetzer, J. Fleig, **Dr. W. Frey**, Dr. Ch. Gusbeth, Dr. A. Heinzel, D. Herzog, Dr. M. Hochberg, Dr. A. Jianu, D. Krust, F. Lindner, DI (Fh) F. Lang, K. Leber, **Prof. G. Müller**, N. Nazarova, I. Papachristou, J. Ruf, **PD Dr. M. Sack**, Dr. G. Schumacher (Guest), Dr. H. Shi, Dr. A. Silve, A. Sivkovich, DI R. Sträßner, **Dr. A. Weisenburger**, R. Wüstner, Y. Zhang, T. Zhang (DFG-PhD student), W. Zhen (CSC-PhD student)

Journal Publications

Bai, F.; Gusbeth, C.; Frey, W.; Nick, P. (2020). Nanosecond pulsed electric fields modulate the expression of the astaxanthin biosynthesis genes psy, crtR-b and bkt 1 in Haematococcus pluvialis. Scientific reports, 10 (1), Article no: 15508.

Gorte, O.; Nazarova, N.; Papachristou, I.; Wüstner, R.; Leber, K.; Syldatk, C.; Ochsenreither, K.; Frey, W.; Silve, A. (2020). Pulsed Electric Field Treatment Promotes Lipid Extraction on Fresh Oleaginous Yeast Saitozyma podzolica DSM 27192. Frontiers in Bioengineering and Biotechnology, 8, Article 575379.

Gong, Q.; Ding, W.; Bonk, A.; Li, H.; Wang, K.; Jianu, A.; Weisenburger, A.; Bund, A.; Bauer, T. (2020). Molten iodide salt electrolyte for low-temperature low-cost sodium-based liquid metal battery. Journal of power sources, 475, Art.-Nr.: 228674.

Rajabi, F.; Gusbeth, C.; Frey, W.; Maisch, J.; Nick, P. (2020). Nanosecond pulsed electrical fields enhance product recovery in plant cell fermentation. Protoplasma, 257, 1585–1594.

Arcena, M. R.; Leong, S. Y.; Hochberg, M.; Sack, M.; Mueller, G.; Sigler, J.; Silcock, P.; Kebede, B.; Oey, I. (2020). Evolution of volatile and phenolic compounds during bottle storage of merlot wines vinified using pulsed electric fields-treated grapes. Foods, 9 (4), Article: 443.

Gorte, O.; Hollenbach, R.; Papachristou, I.; Steinweg, C.; Silve, A.; Frey, W.; Syldatk, C.; Ochsenreither, K. (2020). Evaluation of Downstream Processing, Extraction, and Quantification Strategies for Single Cell Oil Produced by the Oleaginous Yeasts Saitozyma podzolica DSM 27192 and Apiotrichum porosum DSM 27194. Frontiers in Bioengineering and Biotechnology, 8, Article no: 355.

Akaberi, S.; Krust, D.; Müller, G.; Frey, W.; Gusbeth, C. (2020). Impact of incubation conditions on protein and C-Phycocyanin recovery from Arthrospira platensis post- pulsed electric field treatment. Bioresource technology, 306, 123099.

Papachristou, I.; Silve, A.; Jianu, A.; Wüstner, R.; Nazarova, N.; Müller, G.; Frey, W. (2020). Evaluation of pulsed electric fields effect on the microalgae cell mechanical stability through high pressure homogenization. Algal Research, 47, Article no: 101847.

Leong, S. Y.; Treadwell, M.; Liu, T.; Hochberg, M.; Sack, M.; Müller, G.; Sigler, J.; Silcock, P. J.; Oey, I. (2020). Influence of Pulsed Electric Fields processing at high-intensity electric field strength on the relationship between anthocyanins composition and colour intensity of Merlot (Vitis vinifera L.) musts during cold maceration. Innovative food science & emerging technologies, 59, Article No.102243.

3 Safety Research for Nuclear Reactors (NUSAFE): Transmutation -Liquid Metal Technology-

Contact: Prof. Georg Müller

Long-living high-level radioactive waste from existing nuclear power reactors should be transmuted in short-living radio nuclides using fast neutrons provided by a spallation target in an accelerator driven subcritical system or by a fast nuclear reactor. The objective is to reduce the final disposal time of high-level radioactive waste (plutonium, minor actinides) from some 10^6 years down to about 1000 years. Lead (Pb) and lead-bismuth (PbBi) are foreseen as spallation-target and coolant of such devices.

The aim of the institute's contribution is to develop advanced corrosion mitigation processes based on in-situ formation of protective alumina scales especially for parts under high loads like fuel claddings or pump materials in contact with liquid Pb or PbBi. Pulsed large area electron beams (GESA) are used to create aluminum containing surface alloys on steels. In addition, bulk alumina formers like FeCrAl, AFA (alumina forming austenitic steels) and HEA (high entropy alloys) are developed.

All tasks are embedded in European and international projects and cooperations like e.g., ILTROVATORE, MYRTE, GEMMA and EERA-JPNM.

The most relevant results obtained in the reporting period are presented briefly:

3.1 Material development and advanced corrosion mitigation strategies for heavy liquid metal-cooled nuclear systems

Contact: Dr. Alfons Weisenburger

3.1.1 Simulations of flow in the CORELLA facility

Contact: Dr. Renate Fetzer

Within the GEMMA project, corrosion experiments were performed in liquid lead bismuth eutectic (LBE) under flowing conditions in the CORELLA facility. The LBE is confined between an outer stationary cylinder and an inner rotating cylinder. The specimens are placed at a fixed position close to the rotating cylinder. A numerical study was performed to compute the flow field of the LBE for the rotational speeds of the inner cylinder used in the experiments (up to 1200 rpm). Hereby, the free liquid surface deforms under the influence of the centrifugal force and gravity. Taking into account this deformation, the flow field was solved and the velocity around the specimens was determined.

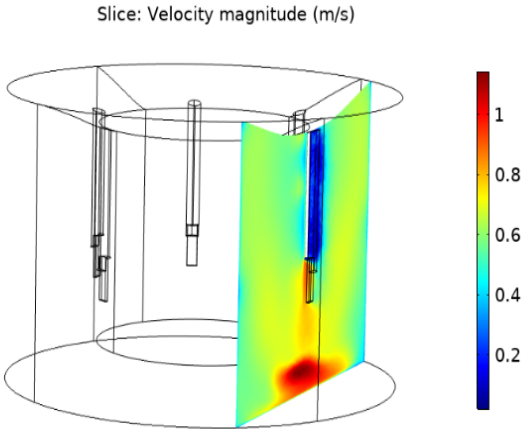

Fig. 3.1.1: Visualization of flow -vertical plane of interest for flow analysis on inner side of specimen 5.

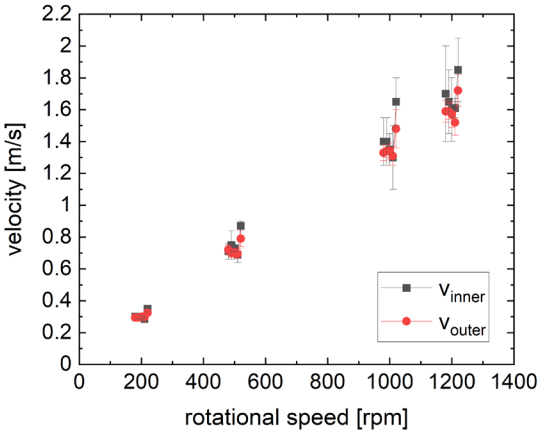

Fig. 3.1.2: Average speed of LBE on inner and outer side of specimens 1 to 5 - plotted versus rotational speed of inner cylinder.

3.1.2 Material development to mitigate corrosion

Contact: Dr. Annette Heinzel

In the frame of the EU project GEMMA corrosion tests in stagnant, oxygen containing Pb up to 10000 h at 480 and 550°C were conducted on samples with alumina or alumina forming coatings, with a TIG weld and on two AFA (alumina forming austenitic) steels. Some of these samples were also tested in the CORRELLA device to explore the influence of flow velocity on the corrosion. All tests are finished and the samples are being investigated.

AFA model alloys with the composition formula Fe-(15.2-16.6)Cr-(3.8-4.3)Al-(22.9-28.5)Ni (wt.%) have shown corrosion resistance to oxygen containing molten Pb at 600°C. By increasing the exposure temperature to 650°C, only the alloy with lower Ni content (~23 wt.%) and minor additions of Nb and Y forms a protective oxide scale. A higher Ni content of ~28 wt.% increases the susceptibility to corrosion attack at 650°C. Minor addition of yttrium facilitates the selective oxidation of Cr and Al and impedes the $Fe(Cr,Al)_2O_4$ formation, which brings a significant benefit to the corrosion resistance of AFA model alloys. Minor addition of niobium increases the Cr availability in austenite, supports the earlier Cr_2O_3 formation, and triggers/enhances the precipitation of B2-NiAl phase, which serves as Al reservoir for the alumina scale formation.

Collaboration: SCK-CEN, ENEA, KTH, SANDIVK, CIEMAT, CEA

Funding: EU-Projects and NUSAFE

Involved Staff

Dr. DP W. An, Dr. R. Fetzer, Dr. A. Heinzel, Dr. A. Jianu, DI (Fh) F. Lang, F. Lindner, Prof. G. Müller, Dr. G. Schumacher (Gast), Dr. H. Shi, A. Sivkovich, **Dr. A. Weisenburger**, Z. Wang (SCS-PhD student)

4 Energy Efficiency, Materials and Resources (EMR): Energy-Efficient Processes -Multiphases and thermal processes-

Contact: Dr. Guido Link

Besides the activities on development of technologies and systems for the plasma heating in the FUSION Program, IHM is also in charge of research and development in the topic Energy Efficient Processes, part of the EMR Program.

An important part of this research is the dielectric characterization of the processed materials in the parameter range relevant to processes under development. Existing test-sets are continuously improved and new test-sets are developed following the new requirements regarding material compositions or process parameter range. Meanwhile a very versatile test lab for dielectric characterization exists. This allows temperature dependent dielectric measurements in the frequency range from 10 MHz to 50 GHz for low as well as high loss materials and from room temperature up to 1000°C for solids, liquids and at pressures up to 20 bar.

All this expertise and the existing industrial scale high power microwave infrastructure faces growing interest from industry and research. Consequently the research group is involved in several national and international joint research projects with objectives in various fields of applications. In the frame of the H2020 Marie Curie international training network TOMOCON a microwave tomographic sensor is under development and first promising experimental result already exist. Within the German-Korean project REINFORCE the potential of microwave dielectric heating has been investigated with respect to energy efficient carbon fiber production. Two more projects have been started in 2018 for the microwave assisted and energy efficient lamination of synthetic leather for automotive industry (e-KOMFORT) and for the microwave assisted intermittent pultrusion of CFRP profiles (IMPULS).

Solid state microwave amplifiers getting more and more competitive compared to magnetron sources with respect to power and costs. Furthermore, such amplifiers allow precise control not only of power level but also of frequency and phase and promise significant longer lifetime than magnetrons. Those features and novel process control concepts might be door openers for novel applications that could not be satisfied with magnetron sources so far. Additionally, those novel microwave source might be useful for microwave sustained plasma generators for plasma activation of CO_2 in the frame of research activities like Power to X. A novel lab for plasma chemistry using atmospheric microwave plasma has been established and will be a major focus towards the MTET Program in PoF IV. First promising results based on novel plasma diagnostic methods have been published. The status of major projects is briefly introduced in the following chapters.

4.1 Plasma chemistry

Contact: Dr. Sergey Soldatov

Conversion of CO_2 into synthetic fuels using microwave sustained plasmas and renewable energies is considered as a promising approach for mitigation of CO_2 emission and energy storage. Among different plasma discharges microwave sustained plasmas have shown to be most efficient for CO_2 splitting into CO and Oxygen. Using pulsed microwave power rather than continuous microwave power may increase the energy efficiency by shifting the thermal equilibrium in the plasma towards vibrational excitation states, which are responsible for the dissociation process. At atmospheric pressure, the nanosecond-scale pulsation of the microwave energy enables a fine control of the gas temperature which opens the opportunity to combine the plasma activation with catalytic one as well as with gas separation membranes.

In collaboration with the Institute for Micro Process Engineering (IMVT) in 2020 our institute explored the reduction of CO_2 in a microwave plasma discharge for its subsequent conversion into valuable chemical precursors and synthetic fuels. By use of advanced optical emission spectroscopy with high spectral and time resolution and the application of novel solid-state high-power microwave generators from our industrial partner HBH microwaves GmbH, for the first time the non-equilibrium state in an atmospheric pressure CO_2 plasma has been revealed (see Fig. 4.1.1). Systematic parameter studies with variation of pulse parameter have shown the benefits regarding increased conversion and energy efficiency as compared to continuous wave operation of the microwave power.

The upscaling towards industrial reactors and tailoring advanced plasma scenarios require more detailed understanding of physics behind. To get this we plan to investigate IR absorption and emission spectra in pulsed microwave CO_2 plasmas with a time resolved FT-IR spectrometry.

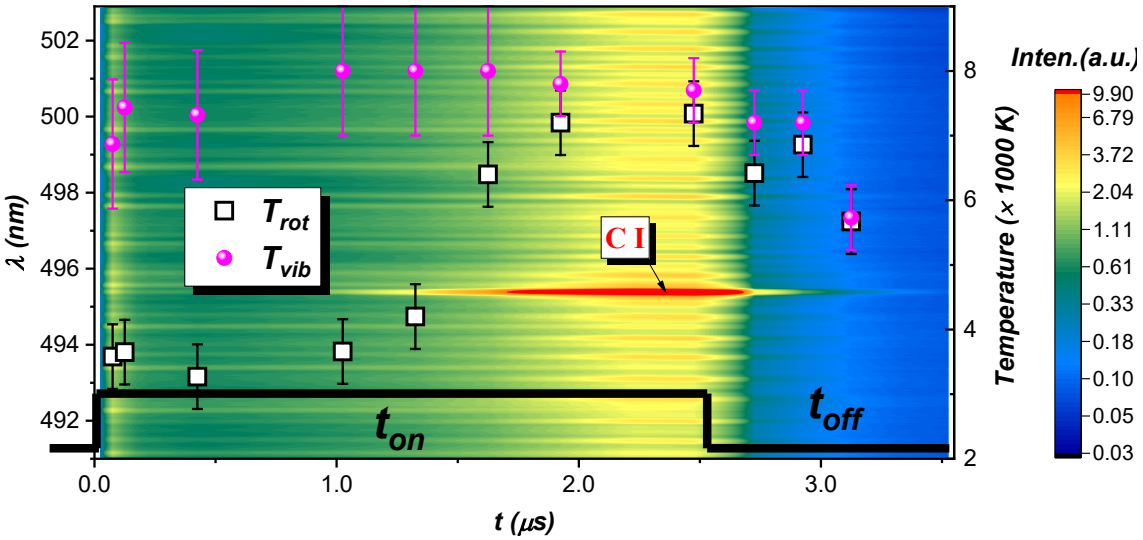

Fig. 4.1.1: Dynamics of microwave CO_2 plasma emission and related rotational (T_{rot}) and vibrational (T_{vib}) temperatures in a pulse scenario with t_{on}=2.5 µs, t_{off}= 7.5 µs and CO_2 gas flow of 12 slm [1].

4.2 e-KOMFORT

Contact: M.Sc. Dominik Neumaier

In addition to technical specifications and price-performance ratio, comfort is also increasingly a decision criterion for buying a car. High-quality materials and comfort are the interface to the user and help to implement the new vehicle concepts more quickly. Up to 9 m^2 of technical textiles are installed in cars today, making the car more attractive both visually and haptically. These decorative materials made of textiles and leather have to be laminated to the three-dimensional surfaces, which has so far been a very energy and time-consuming process. The conventional process transfers the heat to activate the adhesive via heat conduction through the surface of the decorative materials or substrate materials. Microwave technology and suitable adhesives can be used to generate the heat directly and selectively in the adhesive which results in significant energy savings of more than 70 % and a higher productivity. The objective of the project is to develop an innovative process and tool technology for the energy-efficient lamination of decorative materials by using microwaves.

In the first step an appropriate measurement setup was developed to characterize the dielectric properties of the adhesive substrate. In cooperation with the project partner Carl Meiser GmbH & Co.KG, this enabled the development of an adhesive that heats up much better by microwaves than the remaining components of the workpiece. In addition, an appropriate microwave cavity was designed, based on the proven hexagonal Hephaistos technology (see Fig. 4.2.1 (left)). In the design process, loop antennas with different polarizations were used in order to have as many degrees of freedom as possible, which are used to heat the adhesive in the workpiece in the most homogeneous way that is possible. The cavity designed in the simulation was built up (see Fig. 4.2.1 (right)). Four solid-state microwave generators operating in the frequency range from 2.4 GHz to 2.5 GHz act as microwave sources. The advantage of these sources is that the temperature distribution in the adhesive can be homogenized much better than with classical magnetron oscillators. An optimization-based algorithm was developed which controls the frequency, phase and amplitude of the microwave generators in such a way that the temperature distribution in the workpiece is as uniform as possible.

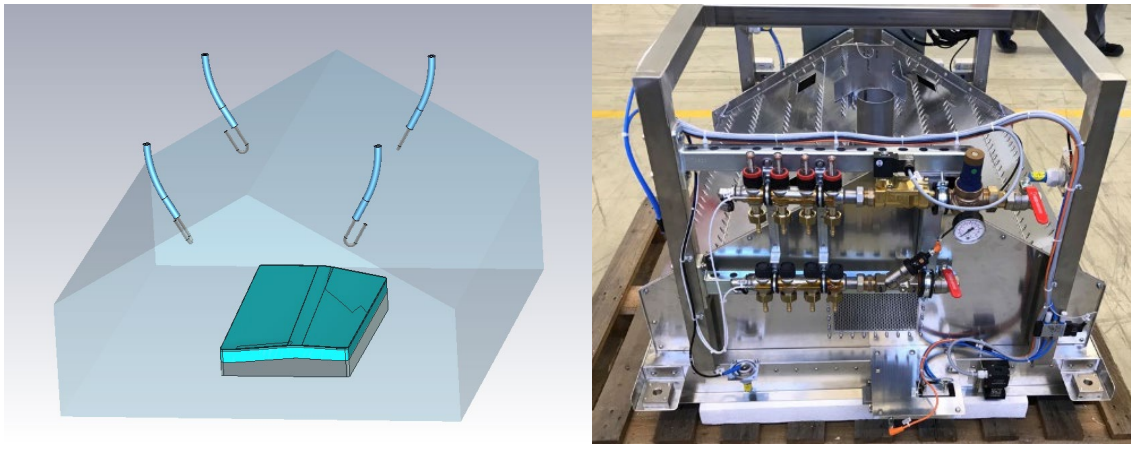

Fig. 4.2.1: Designed microwave cavity (left); Real microwave cavity (right).

Funding: 6th Energy Research Programme of the Federal Government, support code 03ET1576A

4.3 High power solid-state microwave generators

Contact: M.Sc. Dominik Neumaier

Microwave heating has become of increasing interest to industry in the last 2 to 3 decades, because thermal processes can be performed much faster and more energy efficient than with conventional methods that use convection and/or radiation heating for this purpose. In addition, the microwave technology enables material-specific selective heating. However, it's still a major challenge to heat the product homogeneously in a microwave cavity operating at an industrial scale. Therefore, the aim of this project is to improve dielectric heating to become more homogeneous and to develop the necessary microwave sources to extend the use of microwaves to a lot of industrial processes. In cooperation with the company HBH Microwave GmbH (HBH) a novel high-power solid-state generator (1 kW, 2.4 GHz - 2.5 GHz) was developed. This novel microwave generator increases the degrees of freedom compared to a classical magnetron oscillator by providing precise control of amplitude, frequency, and phase. In addition, the generator can also generate very fast pulses with a minimum pulse length of 10 ns (see chapter 4.1).

An experimental setup on an industrial scale, which can handle up to 10 microwave sources, was built up (see Fig. 4.3.1 (a)) to demonstrate the advantages of this new technology. The cavity is a hexagonal structure with a circumferential diameter of 1 m and a depth of 1 m. The microwave energy is coupled into the cavity using slotted waveguide antennas with two different polarizations orthogonal to each other. Inside the cavity the temperature distribution of any workpiece is monitored by an infrared camera. The high-power generators of HBH can directly measure the forward and reflected microwave power over the whole frequency band (2.4 GHz to 2.5 GHz). It makes it possible to measure the resonance frequencies inside the cavity and also detect the resulting temperature profile of each resonance frequency (see Fig. 4.3.1 (b)). In addition, the microwave sources provide synchronized and very fast control of frequency, phase and amplitude in a 1ms cycle. A significant improvement in temperature homogeneity was achieved by using an optimization-based control algorithm that can process several different combinations of the manipulated variables far below the thermal time constant of the workpiece (see Fig. 4.3.1 (c) & (d)).

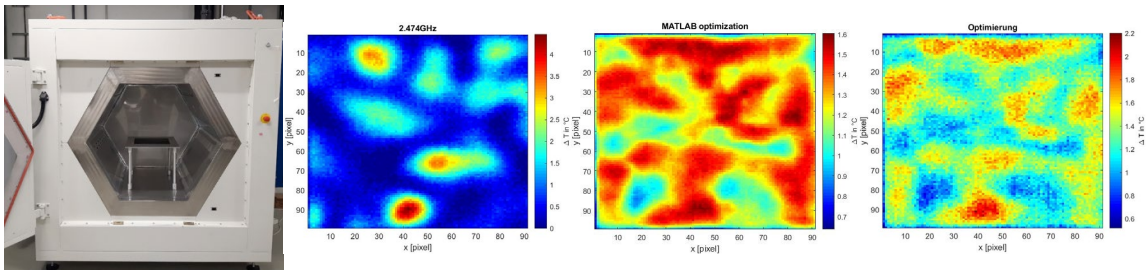

(a) (b) (c) (d)

Fig. 4.3.1: (a) Microwave cavity; (b) measured temperature profiles at a single frequency (out of 65); (c) Optimized temperature profile (virtual superposition of 65 resonance frequencies); (d) Measured optimized temperature profile.

Funding: ZIM cooperation project, support code ZF4204602PR6

4.4 Energy-efficient production of robust carbon fibers (REINFORCE)

Contact: M.Sc. Julia Hofele

Carbon fibers are widely used in lightweight applications, but the carbon fiber production is rather expensive and energy intensive compared to the production of aluminium and steel. Microwave heating has the benefit of heating in the volume and thus may lead to faster and more energy efficient heating rates. A major goal of the project is to research the production of carbon fibers with dielectric heating.

A new fiber winding system was put into operation. The old measurement setup was included to allow the use of the 915 MHz cavity as well as the 2.5 GHz cavity, see Fig. 4.4.1. A first result of a partially stabilized polyacrylonitrile (PAN) fiber achieved with microwave assisted heating can be seen in Fig. 4.4.2. The volumetric heating of the microwave explains very well the darker color in the middle of the fiber. In order to get a better understanding of the thermal runaway effect, which leads to burning the fiber, a mathematical model was setup. The model allows calculating the temperature development along the length of the fiber depending on the fiber speed, air temperature and microwave power. A next step is to verify the model with the experimental setup to determine the process parameters that lead to a stable and controllable temperature profile and the desired degree of conversion. The degree of conversion can be determined with the help of FTIR absorption spectroscopy. FTIR measurements are planned to be used determining the link between stabilization degree and dielectric properties.

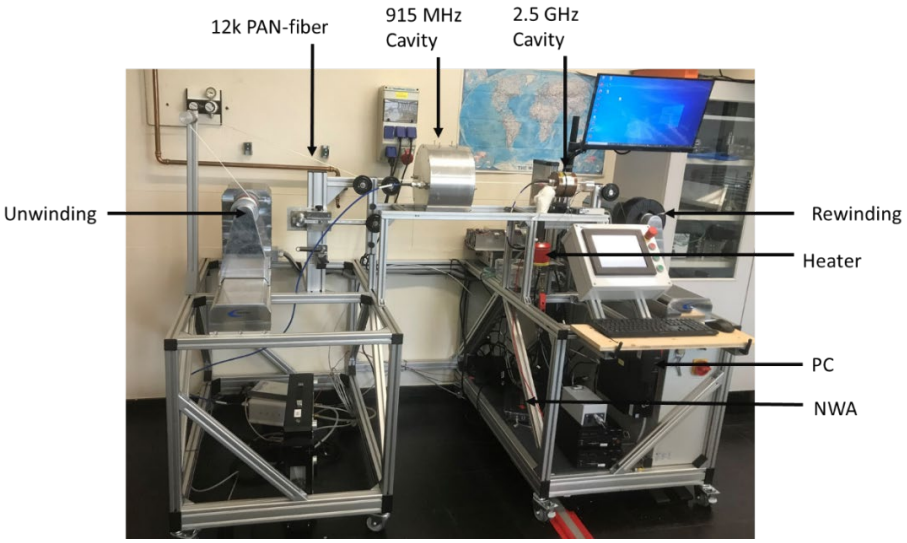

Fig. 4.4.1: Process system including tension and speed controlled fiber winding, conventional and microwave heating at different frequencies.

Fig. 4.4.2: First result of microwave heated PAN fiber.

Funding: ZIM cooperation project; support code ZF4204603SY7

4.5 Smart tomographic sensors for advanced industrial process control (TOMOCON)

Contact: M.Sc. Adel Omrani Hamzekalaei

The European Marie Skłodowska-Curie Training Network “Smart tomographic sensors for advanced industrial process control” (TOMOCON) joins 12 international academic institutions and 15 industry partners, who work together in the emerging field of industrial process control using smart tomographic sensors. In close collaboration with Chalmers University of Technology and the University of Eastern Finland KIT is engaged in the development of a microwave tomography (MWT) system and its application in microwave drying of porous materials.

This microwave tomography (MWT) system is going to be integrated with a high-power microwave drying system to obtain the targeted moisture distribution inside wet polymer foam. The microwave drying system is equipped with a conveyor belt that enables a continuous drying process. The objective is to dry the foam uniformly. Intelligent control of distributed microwave sources is a possibility that might efficiently address any non-uniform moisture distribution. This requires the *in-situ* and non-invasive measurements of the unknown moisture distribution inside the foam.

A prototype MWT setup consists of 7 WR90 open-ended waveguide antennas connected to an Agilent N5224A VNA with a P9164C 2× 16 USB solid state switch matrix has been designed and has already been set-up for tests and calibration in stationary operation (see Fig. 4.5.1 left). Various models and algorithms to solve the inverse problem have been developed and investigated. First promising results have been demonstrated based on test targets such as a PTFE Teflon sphere of radius 1.25 cm and dielectric constant ϵ_{tef}=2.1 hidden in a PU polymer foam with 8 cm thickness and 50 cm in width (see Fig. 4.5.1 right).

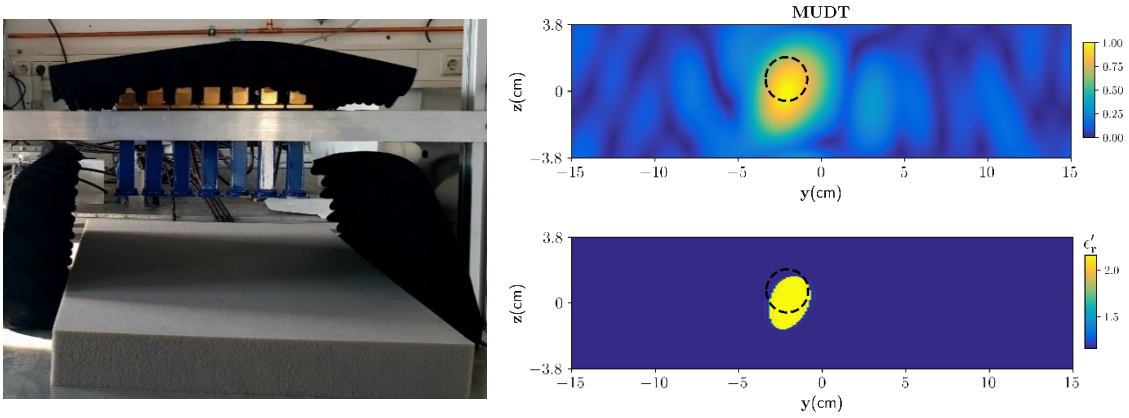

Fig. 4.5.1: Photo of the MWT sensor configuration consists of 7 X-band open-ended waveguide antennas on top of the PU polymer foam and surrounded by absorbers (left). Multistatic uniform diffraction tomography (MUDT) reconstruction (top right) and reconstructed permittivity of the target (bottom right) of a PTFE sphere calibration standard hidden in the polymer foam.

Funding: H2020-MSCA-ITN-2017; Grant agreement 764902

4.6 Innovative microwave pultrusion for the cycle controlled sequential curing of fiber reinforced plastics for modular automated manufacture of complex components (IMPULS)

Contact: M.Sc. Moritz Engler

Pultrusion is a manufacturing process for the production of fiber-reinforced polymer profiles, where reinforcing fibers are impregnated with a thermoset resin and then pulled though a heated die, which cures the resin while imposing the dies profile. The continuous nature of this proces makes it very economical. This process is, however, limited to constant cross section profiles which are straight or of constant radius.

The IMPULS Project aims to develop a microwave powered pultrusion process for the production of carbon fiber-reinforced composite profiles. As the microwave powered pultrusion tool allows to selectively heat the profile in the otherwise cold tool, the degree of cure of the profile can be changed instantaneously by changing the microwave power. By alternating between fully cured and uncured segments, the profile can be locally deformed, opening the process to a variety of new applications. The focus of the IMPULS project lies in developing an applicator with a focus on short transition regions between fully cured and uncured segments.

For this purpose two applicator variants were developed. The first applicator utilizes the local field magnification properties of a double ridge waveguide to focus the heating zone. This applicator has been tested successfully and transition regions of about 1 cm length could be achieved. A second applicator based on a coaxial resonator is currently being constructed.

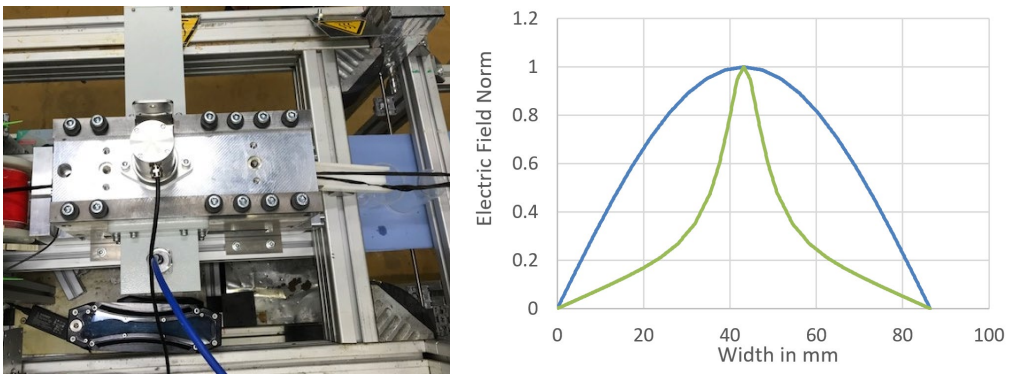

Fig. 4.6.1: Left: Microwave applicator during pultrusion; Right: Normalized electric field strength inside a rectangular waveguide (blue) and a double ridge waveguide (green).

Fig. 4.6.2: Profile produced by the intermittent pultrusion process. The transitional region between the cured section (left) and the uncured section (right) is marked in red.

Funding: BMWi, ZIM Kooperationsprojekt, support code: ZF4204604BL8

4.7 3D Microwave Printing of Composites

Contact: Dr. Nanya Li

Three-dimensional (3D) printing, also known as additive manufacturing, has been developed for more than 30 years for potential application in aerospace, automotive and medical treatment. The 3D printing of carbon fiber reinforced thermoplastic (CCFRP) composites by using the fused filament fabrication method has been liberated from the limitation of classic forming tools and complicated multi-steps preparation. The developed 3D microwave printing system can significantly improve the printing speed compared to the state-of-the-art printing technologies of CCFRP.

The first prototype of a 3D microwave printer SERPENS (Super Efficient and Rapid Printing by Electromagnetic-heating Necessitated System) has been developed and shown in Figure 4.8 (a). The SERPENS equips a small-size coaxial microwave resonant applicator to heat the CCFRP filaments. The applicator was integrated in an upgraded three-axis numerical control machine and is powered by a 300 W, 2.4 to 2.5 GHz solid-state high-power microwave amplifier. A prediction-model based control system was developed to adjust the microwave power to reach a predefined filament temperature during the printing process. CCFRP filaments 0.45 mm in diameter and with the fiber volume content of about 25 %, necessary for the printing process have been produced, as illustrated in Figure 4.8 (b). Looking to the reflection (s_{11}) of the SERPENS printing head, the measured values compare very well with the simulated one. In a well-tuned case reflection coefficient is about -13 dB indicating an efficiency of the applicator of about 95 %. As the continuous carbon fibers are guided into the applicator as an inner conductor of the coaxial resonator and therefore are an essential part of the electromagnetic design, the microwave cannot couple into the applicator without the CCFRP filaments and results in a total reflection, as shown in Figure 4.8 (c).

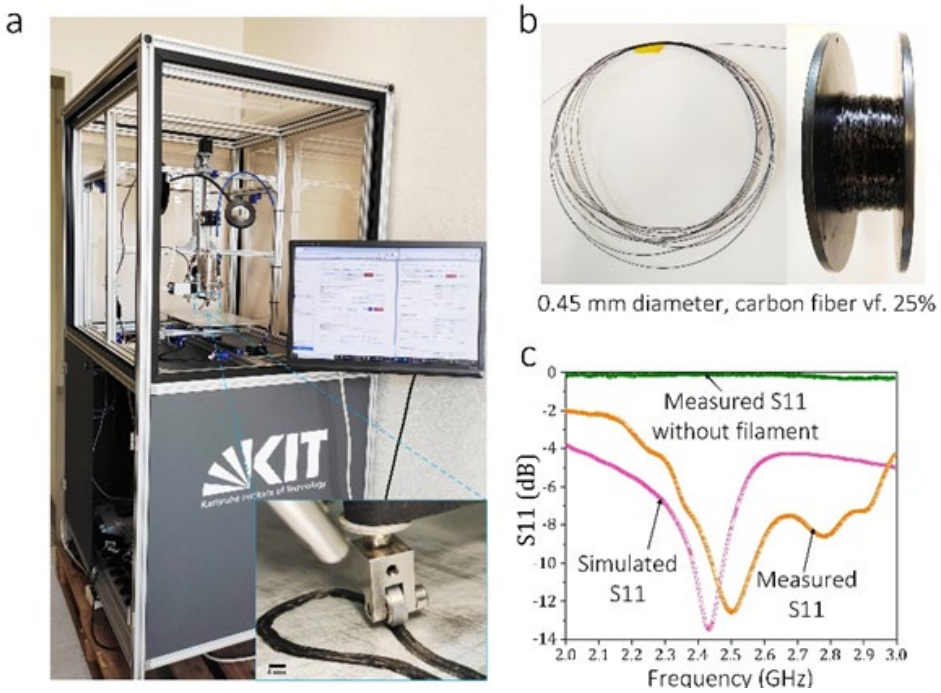

Figure. 4.8: (a) 3D microwave printer SERPENS, (b) impregnated CCFRP filaments, (c) comparison of the simulated and measured S11 of the microwave applicator with or without CCFRP filament.

Funding: Alexander von Humboldt Research Project, YIG Prep Pro

Involved Staff

M. Blekhshtein M. Engler, Frau J. Hofele, Prof. J. Jelonnek, Dr. N. Li, Dr. G. Link, D. Neumaier, V. Nuss, A. Omrani Hamzekalaei, V. Ramopoulos, T. Seitz, S. Soldatov, Frau S. Wadle

Journal Publications

Soldatov, S.; Link, G.; Silberer, L.; Schmedt, C. M.; Carbone, E.; D'Isa, F.; Jelonnek, J.; Dittmeyer, R.; Navarrete, A. (2020). Time-Resolved Optical Emission Spectroscopy Reveals Nonequilibrium Conditions for CO2 Splitting in Atmospheric Plasma Sustained with Ultrafast Microwave Pulsation. ACS energy letters, 6 (1), 124–130.

Zhang, Y.; Ma, Y.; Omrani Hamzekalaei, A.; Yadav, R.; Fjeld, M.; Fratarcangeli, M. (2020). Automated microwave tomography (Mwt) image segmentation: State-of-the-art implementation and evaluation. Journal of WSCG, 2020, 126–136.

Camacho Hernandez, J. N.; Link, G.; Soldatov, S.; Füssel, A.; Schubert, M.; Hampel, U. (2020). Experimental and numerical analysis of the complex permittivity of open-cell ceramic foams. Ceramics international, 46 (17), 26829–26840.

Lähivaara, T.; Yadav, R.; Link, G.; Vauhkonen, M. (2020). Estimation of Moisture Content Distribution in Porous Foam Using Microwave Tomography With Neural Networks. IEEE transactions on computational imaging, 6, 1351–1361.

Li, N.; Link, G.; Jelonnek, J. (2020). Rapid 3D microwave printing of continuous carbon fiber reinforced plastics. CIRP annals, manufacturing technology, 69 (1), 221–224.

Li, N.; Link, G.; Jelonnek, J. (2020). 3D microwave printing temperature control of continuous carbon fiber reinforced composites. Composites science and technology, 187, Article: 107939.

Appendix

Equipment, Teaching Activities and Staff

IHM is equipped with a workstation cluster and a large number of experimental installations: KEA, KEA-ZAR, three GESA machines, eight COSTA devices, one abrasion and one erosion teststand, a gyrotron test facility including a microwave-tight measurement chamber and two teststands for gyrotrons, one compact technology gyrotron (30 GHz, 15 kW CW), several 2.45 GHz applicators of the HEPHAISTOS series, one 0,915 GHz, 60 kW magnetron system, one 5.8 GHz, 3 kW klystron installation and a low power microwave laboratory with several vectorial network analysers.

The project FULGOR, targeting for a renewal of the KIT gyrotron teststand is progressing. In 2013, an agreement on the project structure including the involvement of the KIT project and quality management has been achieved. The final start of the procurement of the equipment was in 2014. The start of operation is expected by end of 2021.

Prof. John Jelonnek has continued to teach the lecture course entitled “High Power Microwave Technologies (Hochleistungsmikrowellentechnik)” for Master students at KIT. Prof. Georg Müller has continued to teach the lecture on “Pulsed Power Technologies and Applications” at KIT. Dr. Gerd Gantenbein has been teaching the part “heating and current drive” of the lecture “Fusionstechnologie B” by Prof. R. Stieglitz, IFRT. Dr.-Ing. Martin Sack hold the lecture course “Elektronische Systeme und EMV” at KIT.

At the turn of the year 2020/2021 the total staff with regular positions amounted to 40 (20 academic staff members, 10 engineers and 10 technical staff member and others).

In addition 16 academic staff members, 2 engineer and 4 technical staff members (and others) were financed by acquired third party budget.

In course of 2020, 1 guest scientists, 13 PhD students (1 of KIT-Campus South, 11 of KIT-Campus North, 1 Scholarship), 2 DHBW student, 4 trainees in the mechanical and electronics workshops worked in the IHM. 1 Master students have been hosted at IHM and 1 Bachelor student and 1 Research internship has been at IHM during 2020.

Strategical Events, Scientific Honors and Awards

M.SC. Laurent Krier received the “Study Award of the SEW-Eurodrive foundation” for his Master Thesis.

Dr. Nanya Li receive the Fellow in the YIG Prep Pro Program of KIT.

Dr. Nanya Li, Dr. Guido Link and Prof. Dr.-Ing. John Jelonnek were honored with 1st place for the Neuland innovation competition.

Dr. Sergey Soldatov received the “Best eposter presentation at the „nanoGe Online conference on Operando characterization of catalysts at work“.

Longlasting Co-operations with Industries, Universities and Research Institutes

- Basics of the interaction between electrical fields and cells (Bioelectrics) in the frame of the International Bioelectrics Consortium with Old Dominion University Norfolk, USA; Kumamoto University, Japan; University of Missouri Columbia, USA; Institute Gustave-Roussy and University of Paris XI, Villejuif, France; University of Toulouse, Toulouse, France, Leibniz Institute for Plasma Science and Technology, Greifswald, Germany.

- Desinfection of hospital wastewater by pulsed electric field treatment in cooperation with University of Mainz and Eisenmann AG.

- Integration of the electroporation process for sugar production with SÜDZUCKER AG.

- Development of protection against corrosion in liquid metal cooled reactor systems in the following EU-Projectes: LEADER, GETMAT, MATTER, SEARCH (Partner: CEA, ENEA, SCK-CEN, CIEMAT).

- Development of large area pulsed electron beam devices in collaboration with the Efremov Institute, St. Petersburg, Russia.

- Experiments on liquid Pb and PbBi-cooling of reactor systems with the Institute for Physics and Power Engineering (IPPE), Obninsk, Russia.

- Development, installation and test of the complete 10 MW, 140 GHz ECRH Systems for continuous wave operation at the stellarator Wendelstein W7-X in collaboration with the Max-Planck-Institute for Plasmaphysics (IPP) Greifswald and the Institute of Interfacial Process Engineering and Plasma Technology (Institut für Grenzflächenverfahrenstechnik und Plasmatechnologie, IGVP) of the University of Stuttgart.

- Development of the European ITER Gyrotrons in the frame of the European GYrotron Consortium (EGYC) and coordinated by Fusion for Energy (F4E). The other members of the Consortium are SPC, EPFL Lausanne, Switzerland, CNR Milano, Italy, ENEA, Frascati, Italy, HELLAS-Assoc. EURATOM (NTUA/NKUA Athens), Greece. The industrial partner is the microwave tube company Thales Electron Devices (TED) in Paris, France.

- Development of a 105 GHz 1 MW gyrotron for the ECRH installation of CEA-WEST tokamak

- Development of Microwave Systems of the HEPHAISTOS Series for materials processing with microwaves with the Company Vötsch Industrietechnik GmbH, Reiskirchen.